An-Najah National University

Faculty of Graduate Studies

Nanotech-based Filtration for Advanced Treatment of Wastewater

By
Ahmed AL-Khaldi

Supervisor
Dr. Abdel-Fattah Hasan

Co-Supervisor
Prof. Amer El-Hamouz

This Thesis is Submitted in Partial Fulfillment of the Requirements for the Degree of Master of Water and Environmental Engineering, Faculty of Graduate Studies, An-Najah National University, Nablus, Palestine.

2018

Nanotech-based Filtration for Advanced Treatment of Wastewater

By

Ahmed AL-Khaldi

This thesis was defended successfully on 15 / 2 / 2018 and approved by:

Defense committee Members	**Signature**
– **Dr. Abdel-Fattah Hasan/Supervisor**	**…..…….**
– **Prof. Amer El-Hamouz/ co-Supervisor**	**……**
– **Dr. Tahseen Sayara /External Examiner**	**……**
– **Dr. Hamdallah Bearat /Internal Examiner**	**……**

Dedication

This thesis is dedicated to:

My homeland Palestine... Al-Aqsa Mosque and Jerusalem

An-Najah National University, my second magnificent home...!

My great parents (my father Dr.Mohsen & my grate mom Obyda) who have always loved me unconditionally and whose good examples have taught me to work hard for the things that I aspire to achieve...

My wife (Alaa) who has been a constant source of support and encouragement...

My beloved brothers and sister for their love and support.

For the two little girls (Orjwan & Maria)

My Aunt Maha and my late Grandfather Sameeh

All the people in my life who touch my heart...

Acknowledgements

I would first like to thank my thesis supervisors Dr. Abdel Fattah and Prof. Amer for their unfailing support and assistance.

A special Acknowledgement for the person how tells me that "If you don't trust in your work no one will trust it" .... Thank you Prof. Hamdallah for your support and fro your appreciated notes and corrections.

Many thanks for Dr. Tahseen Sayara for his praiseworthy efforts.

I am also grateful to the following university staff and colleagues: Dr. Iyad Saadeddin, Eng. Hamees Tubeileh, Eng. Odai Judi and Eng. Mohammad Abo-Obaid.

A very special gratitude goes out to Palestinian water authority PWA and Medill east distillation research center MEDRC for providing the partial financial funding for this research.

I owe my deep gratitude to my family members who have supported me along the way.

الإقرار

أنا الموقع أدناه مقدم الرسالة التي تحمل العنوان

Nanotech-based Filtration of Advanced Treatment of Wastewater

أقر بأن ما شملت عليه الرسالة هو نتاج جهدي الخاص, باستثناء ما تمت الإشارة إليه حيثما ورد, وأن هذه الرسالة ككل أو أي جزء منها لم يقدم من قبل لنيل أي درجة أو لقب علمي أو بحثي لدى أي مؤسسة علمية أو بحثية

Declaration

The work provided in this thesis, unless otherwise referenced, is the researcher's own work, and has not been submitted elsewhere for any other degrees or qualifications.

Student's Name: **اسم الطالب:**

Signature: **التوقيع:**

Date: **التاريخ:**

Table of Content

Dedication III
Acknowledgements IV
Declaration V
Table of Content VI
List of Figures VIII
List of Tables XI
List of Abbreviations XII
Abstract XIII
Chapter One 1
Introduction 1
1.1 General introduction 2
1.2 Status of wastewater treatment facilities in Palestine 3
1.3. Objective and research question 4
Chapter Two: Literature review 5
2.1. Waste water filtration 6
2.2 Activated carbon synthesis and applications in environmental clean up 10
2.3. Synthesis and application of the nano catalyst 16
Chapter Three: Methods and materials 21
3.1. Synthesis of activated carbon (AC) from olive stone (OP) 24
3.2. Characterization of the produced activated carbon AC 25
3.3. Synthesis of zinc oxide (ZnO) nano photo catalyst (NPC) 30
3.4. Ability of synthesized zinc oxide nano photo catalysts naked and supported powder in treating secondary wastewater 32
3.4. Chemical Oxygen Demand (COD) testing method 34
3.5. Pre-depositing of synthesized Nano materials on the surface of the AC filtration media 35

3.6. Pre-depositing of synthesized Nano materials on the surface of crushed glass 36
3.7. Scanning electron microscopy test (SEM) 37
3.8. X-ray diffraction test (XRD) 39
Chapter Four: Results and discussion 41
4.1. Characterization of the produced Activated carbon 42
4.2. SEM - characterization of the produced Zinc oxide nano-catalysts 46
4.3. XRD- characterization of the produced Zinc oxide nano-catalysts 56
4.4. Photo catalytic degradation ability using different types of synthesized zinc oxide powders 62
Conclusion and recommendations 70
References 73
الملخص ..... ب

List of Figures

Figure 2.1: filtration mechanisms in the fixed bed filtration media. Source: Davis, 2010 7
Figure 2.2: Schematic for principle of photocatalysis (Joher et al, 2015).. 17
Figure 2.3: Difference between doped and not doped nano catalyst 19
Figure 3.1: Adopted methodology ..... **Error! Bookmark not defined.**
Figure 3.2: Soaking of olive stone in hexane 24
Figure 3.3: the used tube furnace and the produced activated carbon 25
Figure 3.4: Filtration of the Iodine solution. 28
Figure 3.5: Illustration diagram for iodine number 28
Figure 3.6: Grinding the precipitate precursor to fine powder using agate mortar and pestle 31
Figure 3.7: Sketch for the designed batch reactor 33
Figure 3.8: Constructed batch reactor containing two batches running simultaneously 33
Figure 3.9: The used UV-vis. Spectro-photometer 34
Figure 3.10: Pre-depositing processes of nano ZnO on the surface of the synthesized AC, A) AC and nano zinc oxide wet mixture, B) Mixing on hot plate, C) Dry slurry before calcination, D) Final calcined AC/NPC particles. 36
Figure 3.11: The innovated glass filtration media, before and after pre-depositing the NPC 37
Figure 2.12: The used SEM. 38
Figure 3.13: Rigaku-Miniflex 600 XRD diffractometer 39
Figure 3.14: Preparing the NPC sample for the XRD test 40
Figure 4.1: Particle size distribution for the produced AC 42
Figure 4.2: Forces that affect the filtration media and cause slight movement to its grains 44

Figure 4.3: Plot of C_{max} vs. $C_{max}/N_{m.}$ 45
Figure 4.4: Plot of Resedual concentration vs. $C_{max}/N_{m.}$ 46
Figure 4.5: Nano catalysts produced from graded quality of zinc sulfate heptahydrate. ..... **Error! Bookmark not defined.**
Figure 4.6: Nano catalysts produced from commercial quality of zinc sulfate heptahydrate. ..... **Error! Bookmark not defined.**
Figure 4.7: Average particle size of the nano catalysts produced from graded and commercial quality of zinc sulfate heptahydrate. ..... **Error! Bookmark not defined.**
Figure 4.8: Nano ZnO catalysts produced from commercial quality of μ-ZnO..... **Error! Bookmark not defined.**
Figure 4.9: Average particle size of the nano catalysts produced from graded and commercial quality of zinc sulfate heptahydrate. ..... **Error! Bookmark not defined.**
Figure 4.10: Graded quality of micro Zinc Oxide.**Error! Bookmark not defined.**
Figure 4.11: Commercial quality of micro Zinc Oxide.**Error! Bookmark not defined.**
Figure 4.12: X-Ray diffraction pattern for nano ZnO produced from commercial ZnSO4.7H2O 56
Figure 4.13: X-Ray diffraction pattern for nano ZnO produced from graded ZnSO4.7H2O. 57
Figure 4.14: Diffraction pattern of X-ray for commercial ZnO and standard Zincate RRUFF ID: R060027.2. 57
Figure 4.15: XRD pattern of produced ZnO from graded micro-sized ZnO. 59
Figure 4.16: XRD pattern of produced ZnO from commercial micro-sized ZnO..... 59

Figure 4.17: Correction factor for particle size estimated by X-ray diffraction pattern for the synthesized ZnO which was produced from commercial and graded ZSH raw material.....**Error! Bookmark not defined.**

Figure 4.18: Batch experiment for 0.25 mg ZnO catalysis in 100 ml of secondary waste water from Nablus western WWTP. 62

Figure 4.19: Batch experiment for 0.25 g of ZnO catalysis produced from commercial micro-sized ZnO in 100 ml of secondary waste water from Nablus western WWTP. 64

Figure 4.20: The expected effect of Zn^{2+} on COD of the batch experiment, a) ongoing pattern, b) Real pattern neglecting Zn^{2+} effect, c) interpretative effect of the Zn^{2+}..... 65

Figure 4.21: UV absorption at the surface AC particles, green semi-spheres represent the activated NPC and the red one represent not activated NPC due to obstruction of UV beams. 67

Figure 4.22: Photocatalytic activity of G\ nano ZnO (5:1 weight ratio). Each batch contains 1 g of G\ZnO particles and 100 ml of secondary effluent. 69

List of Tables

Table 1: Filters classification according to the material of the filtration media 8
Table 2: Filters classification according to number of used filtration layer and depth of each layer 9
Table 3: Filters classification according to the quality of inflow. 10
Table 4: Activated carbon's preparation methods from olive cake. 15
Table 5: Diameter of the produced ZnO (nm) from commercial and graded raw precursor 58
Table 6: properties of the produced nano ZnO from commercial and graded raw micro sized ZnO 60
Table 7: Nano ZnO catalysts deposition yield for four activated carbon samples 66

List of Abbreviations

AC	Activated carbon.
BOD	Biological oxygen demand.
COD	Chemical Oxygen Demand.
EPA	Environmental Protection agency.
MCM	Million cubic meter.
OPT	Occupied Palestinian territories.
OS	Olive stone; pomace.
PWA	Palestinian water authority.
RSF	Rabid sand filter.
SSF	Slow Sand Filter.
WTP	Water treatment plant.
WWTPs	Wastewater treatment plants.
ZSH	Zinc sulfate heptahydrate
NPC	Nano photocatalysis
NTU	Nephelometric Turbidity Units
SG	Specific Gravity

Nanotech based filtration of advanced treatment of wastewater

By
Ahmed AL-Khaldi
Supervisor
Dr. Abdel-Fattah Hasan
Co-Supervisor
Prof. Amer El-Hamouz

Abstract

In this research a new innovative modification on the traditional tertiary filtration-treatment units using zinc oxide nano photocatalysis is suggested to improve the quality of the treated effluents. The value of this idea lies in using cheap nano materials in modifying the filtration medias which grantee longer operation time with less frequently need for backwash or regeneration of the filtration media what makes the filtration process more sustainable and economically convincing solution.

In this research, the nano zinc oxide catalysis was successfully lab synthesized from high purity graded raw chemicals (99.5%) and also from commercial raw materials (purity $\geq$ 95%). No significant difference in the size of the produced catalysis based on the purity of the raw material. Where, the zinc oxide nano photocatalysis was produced in size of 69 nm from commercial zinc sulfate heptahydrate and size of 29 nm from graded zinc sulfate heptahydrate. In the same manner, nano ZnO catalysis which was produced from commercial micro-sized ZnO have a size of 28 nm which is greater than the nano ZnO catalysis originated from graded raw micro-sized ZnO by just 11 nm.

Photocatalytic degradation ability of the produced nano catalysis was tested in batch experiments as powder or after pre-depositing it on the surface of activated carbon or recycled glass. The nano photocatalysis produced from commercial raw chemicals (ZnSO4.7H2O and micro-sized ZnO) shows high degradation ability for the pollutants in the secondary wastewater with efficiency reaches 85% of total chemical oxygen demand (COD) in the powder batch, and exceeds this value to 97% in the batch of pre-deposited nano catalysis on the surface of the recycled glass.

Carbon and recycled glass were tested as nano photo catalysis carrier. The activated carbon didn’t show the sought after results where the nano catalysis easily escaped to the solution in the batch experiment moreover the black imperial structure of the AC obstructed sun light and ultraviolet light which activate the photo catalytic reaction causing deficiency in activation of the nethermost photocatalysis. Unlike AC filtration media, the filtration media made of crushed glass allows the UV to penetrate its structure and therefore activating the pre-doped nano photo catalysis even in the bottom layers of it.

Finally, the results of this research are the milestone of other researches in order to develop a self-cleaning filtration media.

Chapter One

Introduction

1.1 General introduction

Palestine has one of the lowest available water per capita in the region (PWA, 2014), Palestine suffers extreme water shortage due to constraints imposed by the conditions of Oslo and second Oslo agreements, with accessible fresh water of less than 70 cubic meters per capita annually. The World Business Council for Sustainable Development defines the limit of water scarcity "below 1,000 cubic meters per capita per year at which water scarcity begins to hamper economic development and human health and well-being" (WBCSD, 2005). Thus, the adoption of the integrated water resources management approach and the mobilization of all additional conventional and non-conventional water resources are needed. Therefore, the re-use of reclaimed treated wastewater for industrial and agricultural purposes is an important goal. Treated wastewater is seen as one of the promising solutions that can assist in partially filling the gap of the growing needs for water in Palestine (PWA, 2012), knowing that most of the irrigated agriculture in Palestine depends on available fresh water, and consumes about 50% of all extracted groundwater (110 MCM annually).

Growing worldwide water demands have carried planers to consider sustainable national water sources. And this is through with the pressing need of solutions for the aggravating wastewaters' problems.

1.2 Status of wastewater treatment facilities in Palestine

In case of completion of all wastewater treatment projects in Palestine; an annual wealth of more than 90 MCM of treated wastewater is expected (49M MCM from the West Bank WWTPs and 48 MCM from Gaza WWTPs) compared to current 54 MCM (17 MCM from WB WWTP and 37 MCM partially treated from the Gaza WWTP). Indeed, reuse of this wastewater could fill a considerable gap of water demand for the agricultural sector. But this solution couldn't be applied due to the low quality of effluents of all operated WWTPs in Palestine especially in Gaza strip except the one in Al-Bireh city with flow less than 2 MCM and scattered WWTP in Gaza strip produce around 1 MCM. The organic pollution of this 90 MCM (before treatment) is expected to be more than 40,000.0 ton/year with removal of just 3000 ton/year. The total nitrogen pollution is expected to be around 7000 ton/year with reduction less than 100 ton/year (PWA, 2012).

The very low quality of the Palestinian WWTPs' effluents is attributed to the heavily contaminated wastewater and the high flocculated inflow. To overcome such problems, two solutions are proposed: the first one is to design and construct new larger primary and secondary treatment units. Otherwise, tertiary or advanced treatment units such as filter are needed.

Indeed, adoption of first solution needs huge budget to cover the substantial capital and operational costs and operational and maintenance efforts to treat the wastewater. Though, the second option is mostly preferred by the sector planners since it will depend basically on already constructed

WWTP (Samhan et al., 2011). This study will focus on the second option. To overcome some common operational complications and problems of wastewater effluent's filters such as successive backwashing and air scoring of filters media, and most importantly the selectivity of filtered contaminants, and the footprint of filters components.

1.3. Objective and research question

In this study the main objective is to develop an innovative filtration media which can be used in the Palestinian WWTPs to treat the secondary effluents of these plants and achieve the strict Palestinian standards which will enhance the capability for using the Palestinians WWTPs' effluents in the agricultural sector. To achieve the main objective of this research the next sub-objectives are determined:

1. Synthesis of the selected nano photo catalyst.
2. Testing the produced nano photo catalyst ability to degrade real secondary effluent of Palestinian WWTP
3. Pre-depositing nano photo catalyst on the novel filtration media for the purposes of continuous auto-degradation of contaminants in the secondary WW effluents.

Research question

Will the new filtration medium with nano photo catalysts pre-deposited on its surface be able to decompose contaminants of secondary effluent and produces effluent that meets the Palestinian standard, with no or less backwash frequency for the new filter?

Chapter Two
Literature review

2.1. Waste water filtration

No doubt, wherever humans have used fluid, often they have used filters. The simple principle of filters makes it easy to be used in several purification cases. In addition, its high efficiency and low capital and operational cost make it the most popular conventional treatment process (Tchobanoglous et al., 2012). Filtration is a very widely used process, from the tap filters to the modern advanced membrane filters.

Generally, filtration is a process where the fluid flows through permeable media for the purposes of perfection and impurities removal. In Wastewater filtration the pre-treated wastewater flows through porous media like sand, activated carbon and crushed granite, for removal of suspended solids, biochemically decomposition of the organic matter, and killing the pathogenic microorganisms (Davis, 2010).

2.1.1. Mechanisms of filtration MOF

The dominant filtration mechanism in the slow sand filters SSF is the mechanical screening Fig (2.1-a), where the particles have diameter greater than the smallest opening of the filtration media. This process forms a cake of contaminant on the top surface of the filtration media which could increase the efficiency of contaminants and micro-organism removal. On the other hand it decreases the flow rate and increases the head loss.

Water momentum decreases when flowing through the porous media. That makes the water streamline passing the space between the granular particles with low speed. This allows the larger particles to settle on the

filtration media granules in the short distance in the pores of the porous filtration media Fig (2.1-b).

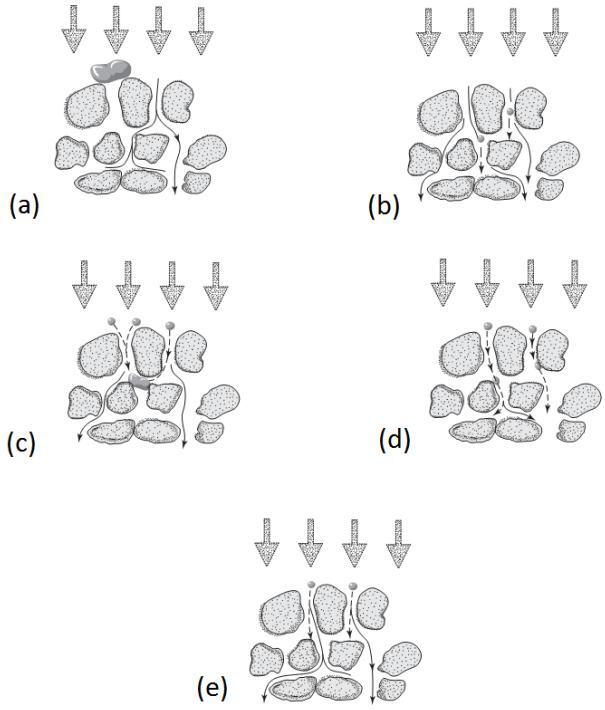


Figure 2.1: filtration mechanisms in the fixed bed filtration media. Source: Davis, 2010

The water streamline flows around the rounded granules of the filtration media, which brings the contaminants particles to attach to each other due to the rotational momentum. That prevents the new larger particles from being released through the filtration media by screening Fig (2.1 -c). The small contamination particles could be intercepted or adsorbed because of the bended water-flow around the filter granules, which allow these particles to pass close enough to the detaining filter's granules Fig (2.1-d). Particles with sufficient mass to release from the rotational movement of the stream line continue the movement in tangential straight line counters to the original bended motion Fig (2.1 -e) (Davis , 2010).

2.1.2. Types of filters (filters classification)

Filters could be sorted according to the material of the filtration media into five types: garnet, ilmenite, sand, anthracite, and granular activated carbon AC. Table 1 shows specifications for each of the filtration material type (Tchobanoglous et al., 2012).

Filters could be calcified according to the number of the different used layers of filtration media into five types; single media (monomedia), deep bed monomedia, dual media, deep bed dual media and mixed media. The Table 2 shows the filter classifications based on the number of used layers.

Table 1: Filters classification according to the material of the filtration media

Property	Unit	Garnet	Ilmenite	Sand	Anthracite	GAC
Effective size, ES	mm	0.2–0.4	0.2–0.4	0.4–0.8	0.8–2.0	0.8–2.0
Uniformity coefficient, UC	UC	1.3–1.7	1.3–1.7	1.3–1.7	1.3–1.7	1.3–2.4
Density, ρ_p	g/mL	3.6–4.2	4.5–5.0	2.65	1.4–1.8	1.3–1.7
Porosity, ε	%	45–58	N/A	40–43	47–52	N/A
Hardness	Moh	6.5–7.5	5–6	7	2–3	Low

Table 2: Filters classification according to number of used filtration layer and depth of each layer

Filter Classification	Number of the used filtration media	Filtration media/s used	Depth of the used filtration media/s (m)
Monomedia	1	Sand	0.6-0.76
Deep-bed monomedia	1	Anthracite or granular activated carbon GAC	1.5-1.8
Dual media	2	Anthracite or GAC and sand	0.45–0.6 of anthracite or GAC over 0.23–0.3 of sand
Deep-bed Dual media	2	Anthracite or GAC and sand	1.5-1.8 of anthracite or GAC over 0.23–0.3 of sand
mixed media	3 or more	Anthracite as the top layer, sand as the middle layer, garnet or ilmenite as the bottom layer.	0.45–0.6 anthracite 0.23–0.3 sand 0.1–0.15 garnet or ilmenite
Source: Tchobanoglous et al., 2012			

Rapid filters also could be classified according to the quality of inflow to four types: conventional filtration, direct filtration, in-line filtration (contact filtration) and two-stage filtration. In general, the turbidity in NTU unit is used to indicate the inflow and out flow of the filters. Table 3 shows the description of each sort.

Table 3: Filters classification according to the quality of inflow.

Classification of rapid filters according to pretreatment level	Inflow turbidity (NTU)	Description
Conventional filtration,	For high turbidity	Coagulation utility followed by flocculation tank after that secondary sedimentation tank are required before the filtration
Direct filtration,	<15	Coagulation flocculation utility is provided before the filtration
In-line filtration (contact filtration)	<10	Just coagulation is required before filtration by adding chemical coagulant
Two-stage filtration	<100	Coagulation unit followed by roughing filter is provided before filtration
Source: Tchobanoglous et al., 2012		

2.2 Activated carbon synthesis and applications in environmental clean up

2.2.1. Historical overview

The activated carbon is “a solid, porous, carbonaceous material prepared by carbonizing and activating organic substances. The raw materials, which include sawdust, peat, lignite, coal, cellulose residues, coconut shells, petroleum coke, etc., may be carbonized and activated at high temperature with or without the addition of inorganic salts in a stream of activating gases such as steam or carbon dioxide. Alternatively, carbonaceous matter may be treated with a chemical activating agent such as phosphoric acid or zinc chloride and the mixture carbonized at an elevated temperature,

followed by removal of the chemical activating agent by water washing" (FAO / WHO 2010).

The use of carbon as sorbent is ancient as the history is. The doctors of Egyptians and Sumerians were the first known user of the carbon before 3500 B.C. It was used for the medical applications (Inglezakis and Poulopoulos, 2006). In 1500 B.C Egyptians used carbon in adsorption of fetid-smell vapors from decayed wounds. Ancient Greek used another medical application of carbon where it was used to reduce the effect of food poisoning by adsorption of the excretory poisons of the bacteria in the intestinal tract. (Bandosz, 2006; Cecen and Aktas, 2012).

The first use of carbon for the water treatment is not new and back to 450 B.C when the Indians use the charcoal and sand filters to purify their water. Later on in 200 AD, the Sanskrit people write down one of the earliest text that describes the water-filtration process. Among the history the carbon was used for medical purposes, reduction of ores in bronze manufacturing, odorous vapors adsorption, water purification and sugar syrups decoloring. But it was produced in relatively small quantities at local scale. Activated carbon industry was appearing at the beginning of the twentieth century (Cecen and Aktas, 2012).

The unique properties of the activated carbon and the relative low production and regeneration cost make it a good option for tertiary treatment of secondary effluents of the WWTPs. Such additional treatment step is generally required when the secondary effluent dos not achieve the treatment standards.

2.2.2. Synthesis of the activated carbon

Activated carbon can be produced from any materials with high concentration of carbon. This transformation could be due to physical, chemical, or chemo-physical process. (Ansari and Khan, 2009)

Olive stone is good candidate to be used as precursor for the activated carbon since it is a carbonious material with high concentration of carbon. Indeed, the olive stone is carbonaceous material with more than 85% of composition is carbon (Youssef et al., 2006; Moreno-Castilla et al., 2001).

Raw organics with intense carbonic texture can be transformed to carbon by heating it in absence of oxygen, this physical or thermal process could be done under flow of an inert gas like N_2, CO_2 and H_2O which increases the micro porosity in the produced carbon surface. (Blasi, 2008) (Margaret et al., 1973)

Chemical activation of carbon necessitates pre-treating it with chemical activation agent to achieve the smallest size of pores on the surface of the carbon and therefore the highest surface area and adsorption capacity.

Several chemical activation agents could be used like potassium hydroxide KOH (Ubago-Pérez et al., 2006; Martinez et al., 2006), phosphoric acid H_3PO_4 (Yakout et al., 2011), zinc chloride $ZnCl_2$ (Yahia, 2006; zyoud et al., 2015) and others, table 4 summarize some previous works on Olive stone activation.

Among all these activation agents the $ZnCl_2$ is considered the most common activation agent (Uğurlu et al., 2008). Where, the soaking of AC's precursor with $ZnCl_2$ increases the uniform micro porosity of the produced

AC. Different from $ZnCl_2$ the other common activation agents like KOH and H_3PO_4 could provide high surface area but with much less uniformity that could obstruct the deep absorption of the smallest molecules or particles (Molina-Sabio & Rodriguez-Reinoso, 2004).

3.2.3. Applications of Activated carbon

Activated carbon has long been used as sorbent for various contaminants, even in low concentrations (Molina-Sabio & Rodriguez-Reinoso, 2004; Berger, 2012). Indeed, activated carbon applications are based on its sorption properties (adsorption, absorption and ion exchange). Certainly, in the case of chemically activated carbon the surface adsorption plays the main role among the sorption mechanisms (Cecina and Aktas, 2011; Alaya et al, 2000).

The activated carbon produced from redundant agricultural waste materials was wildly studied. Notably, it could be produced from abundant agricultural by-products like olive stone (see Table 4) for phenol, heavy metal and organics adsorption (Bohli et al., 2015; Babakhouya et al., 2010), rice husk (Rahman et al., 2005) for copper adsorption, sugar cane (Bernardo et al., 1997) for organic dye removal, almond shell and pecan shell (Bansode et al., 2003) for VOCs adsorption, oil palm (Wirasnita et al., 2014) for endocrine disrupting chemicals adsorption.

Interestingly, the type of the granular activated carbon GAC and the contact time between the contaminated sample and the GAC have no significant effect (Choi et al., 2006).

Activated carbon could be produced from non-conventional waste like plastic PPT (Yuliusman et al., 2017) which could be used for natural gas storage. Tires also had been used as precursor for the activated carbon (Butt et al., 1998) (Gupta et al., 2013; Yaghmaeian et al., 2015) for water purification and mercury adsorption; the tires AC also could be used in tertiary treatment of municipality and industrial wastewater (Lin and Teng, 2002). Activated carbon produced from sewage sludge has been tested for adsorption of a lot of contaminants like Mercury (zang et al., 2005), copper ion and phenolic EDSs (Nuhu et al, 2017), oxalic acid (Huang et al., 2017), organics (Otero et al., 2003). A detailed information about reuse of the waste materials for activated carbon production could be found in Dias et al. review (Dias et al., 2007) and Alslaibi et al. review (Alslaibi et al., 2012)

Table 4: Activated carbon's preparation methods from olive cake.

Activation agent (A.A)	*Impregnation ratio (by weight) AA:OS*	*soaking time(h)*	*Activation temp.*	*Heating rate ˚C/min*	*Activation time(h)*	*Atmo-sphere*	*Flow rate ccm/min*	*Yield%*	*BET surface area m2/g*	*Reference*	*Year*
KOH	1:1	3	900	-	1	N_2	-	20.21	-	Martínez et al.	2006
KOH	2:1	12	800	10	3	N_2	300	24	957	Ubago-Pérez et al.	2006
KOH	1.25:1	24	600	10	2	N_2	150	39.5	915.4	Alslaibi et al.	2013
KOH	0.5:1	3	800	-	2	N_2	300	-	1500	Moreno-Castilla et al.	2001
NaOH	3:1	6	700	20	01:30	N_2	100	64.8	1524	Martins et al.	2015
H3PO4 (80%)	2:1	4	500	3	2	N_2	200	31	1218	Yakout et al.	2016
H3PO4	-	9	410	-	02:30	N_2	-	-	1040	Bohli et al.	2015
H3PO4 (75%)	2.4:1	-	500	10	1	N_2	300	-	336	Moreno-Castilla et al.	2001
H3 PO4	-	7	410	-	8	N_2	-	-	1285-1421	Nouri and Ouederni	2013
H3PO4 (85%)	1.2:1	3	500	5		N_2	20	34	738	Jaouadi et al.	2017
HNO3	3:1 (v/v)	12	900	-	1	N_2	-	-	620	Youssef et al.	2006
HNO3 (1 M)	5.56:1	4	410	-	02:30	N_2	-	-	925	Bader et al.	2014
HNO3 (15 M)	13.3:1	24	550	5	00:30	vacume	-	-	1400 ~ 1700	Haydar et al.	2003
ZnCl2	2:1	8	850	5	-	N_2	-	-	1150-1917	Gonzalez et al.	1978
ZnCl2	2:1	12	500	-	1	N_2	-	-	1291	Solara et al	2008
ZnCl2 (20%)	5:1	24	450	30	2	N_2	500	47.4	1480	zyoud et al.	2015
ZnCl2 (20%)	-		650	-	2	N_2	150	54.8	790.25	Uğurlu et al.	2009
H2SO4	1.8:1	24	500	5	-	N_2	20	34	94	M.Jaouadi et al.	2016
CaCl (7%)	-	7	824	-	7	CO2	100	-	670	Juárez-Galán et al.	2009

2.3. Synthesis and application of the nano catalyst

Since Fujishima and Honda (Fujishima and Honda, 1972) discovered the photolysis of water at the surface of TiO_2 electrode, the researchers, research centers and scientific institutions give a growing concern to the promising research domain (Jiao et al., 2009).

In a simple manner, nano catalyst is atom, molecule, enzyme or solid surfaces with at least one dimension less than 100 nm, and it also could be in any matter phase of gas liquid or solid (Chorkendorff and Niemantsverdriet, 2017). The main function of the catalyst is to speed up the chemical reaction by decreasing the starting energy required for the spontaneity of the reaction. This could happen by providing stronger bonds with appropriate orientation for the reactants. Catalyst could be as the same phase as the reactants (homogeneous catalysis) like $Cl_{(g)}$ catalyst in ozone decomposition reaction or as different phase of the reactants (heterogeneous catalysis) like the oxidation reaction in the car's exhaust in which the CO(g) is oxidized to CO2 on the surface of solid metal catalyst (Chorkendorff and Niemantsverdriet, 2017) .

2.3.1. Nano photo catalysis

Nano photo catalysts are generally semi-conductors like ZnO, TiO_2, Fe_2O_3 and others. It speeds up the photo reaction by taking the advantages of the energy of the incident light. If the light denoted energy is equal to or greater than the band gap energy (BGE) of the catalyst it will be

enough to provide the electrons in the valance band (VB) with enough energy for excitation to the conduction band (CB) leaving a positive hole(h^+) in the VB. The impulsive electron has the ability to degrade any substrate with lower BGE by reducing it or it can react with electron accepter as O_2 forming super oxide radical $O_2^{-\bullet}$. Simultaneously the hole h^+ in the VB can oxidize organic molecules or forming $OH^\bullet$ radicals by oxidizing OH^- and H_2O molecules. Figure (2.3) illustrates the photo catalytic reaction (johar et al., 2015).

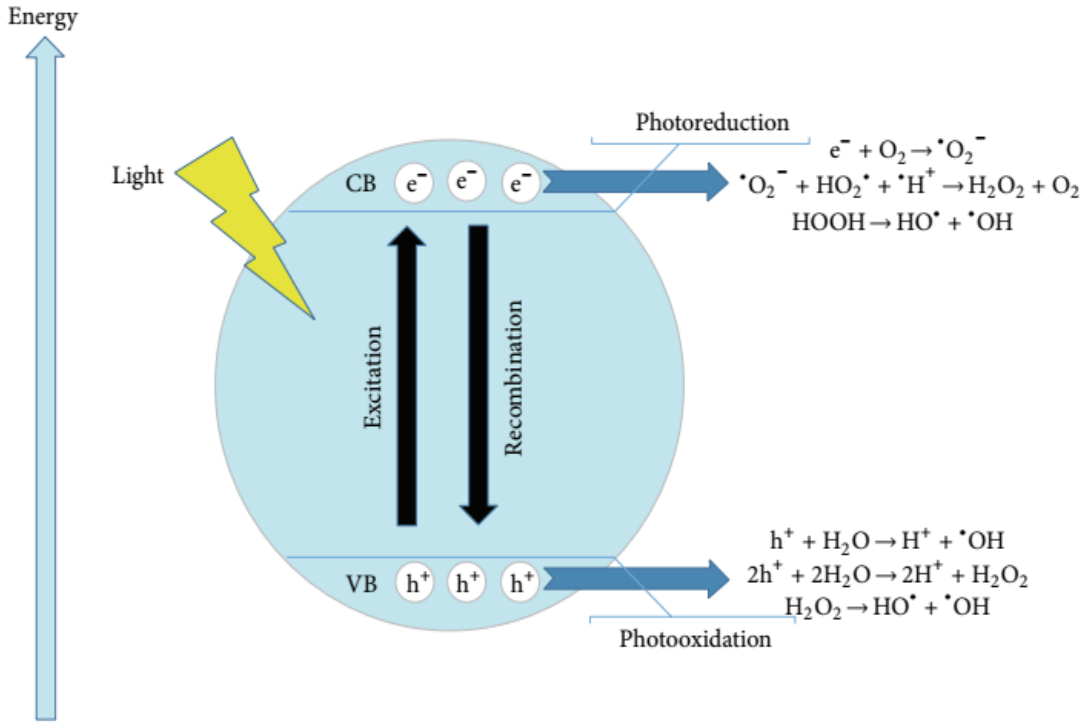


Figure 2.2: Schematic for principle of photocatalysis (Joher et al, 2015).

Photo catalyst could activate the photo reaction when receive the narrow UV light tail in the day light which form less than 3% of the sun light photons 95% of these 3% are ultra violet with the lowest energy level UV-A with wave length between 390-410 nm. Instead of the UV tail;

some nano catalyst like ZnO could be stimulated by the visible light which is considered more economical than the artificial light and easier in the practical field.

2.3.2. TiO_2 and ZnO photo catalysts

Obviously, Titanium dioxide nano photo catalysts were intensively studied (Weir et al., 2012). The special properties of the nano titanium dioxide make it the focus of attention in the last few decays. Titanium dioxide nano photo catalysis is one of stronger photo catalyst with BGE 3- 3.2 eV which gives it a high oxidation and reduction potential making it enough to warrant a degradation of wide range of contaminants (Amet and Ameta, 2017)

The stability, low toxicity, and relatively low cost of the TiO_2 makes it one of the common options in many photo catalytic applications. The high BGE for the naked TiO_2 catalyst is a double-edged sword that could photo degrades a variety of contaminants but also need higher activation energy which requires photons with high energy and short wavelength less than 387 nm.

This limitation on the wavelength which is required to activate the TiO_2 photo catalyst $_{\text{makes}}$ the final application of it $_{\text{more}}$ expensive since it needs an artificial source for intense UV light to replace the narrow and weak UV tail in the sun light spectrum (4 to 7% of the whole sun light). Indeed, the photo catalytic reaction of the TiO2 could go spontaneously under sun light in case of pre-coupling it with other dopant which should have smaller BGE to oxidize and evicts the valance electrons by energy of the visible light photon. See Figure (2.4).

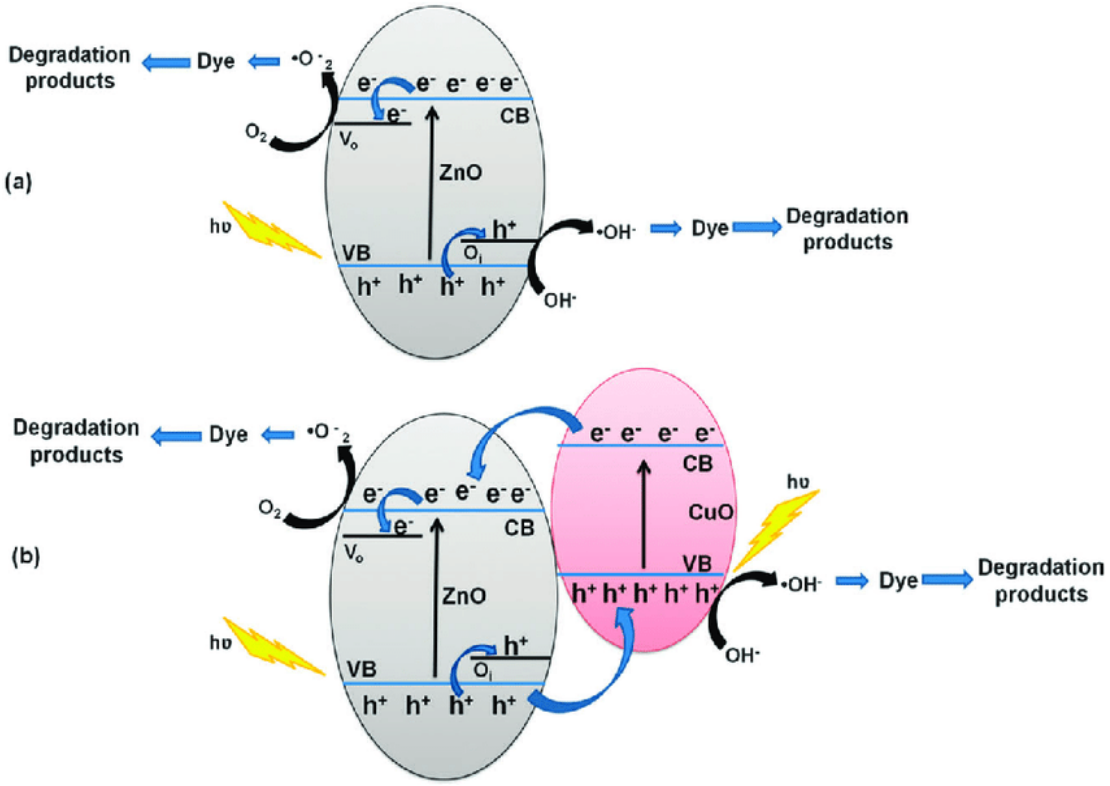


Figure 2.3: Difference between doped and not doped nano catalyst

2.3.3. Nano-Catalysis in the field of application

Nano-catalysis was tested in purification of water and wastewater and appear promising solution. The reviews of Prachi et al (2013), Lens et al. (2013) and Chokshi & Bora (2014) discuss the application of Nanotechnology in wastewater treatment and provide examples for successful experiments that used the nano catalysis in removing organic pollutants, heavy metals such as arsenic, lead, mercury, copper, cadmium, chromium and nickel. Degradation of microbial contaminants like E.coli using ZnO and TiO2 is also discussed.

Nano photo catalysis was tested in various treatment applications; The ZnO-nano coated electrodes decompose more than 60 % of the

perfluorinated compounds in the effluents of wastewater treatment plant (Zhang et al., 2016).

Chemical oxygen demand (COD) of real waste water and textile dye were reduced to 43.3% and 100% by simple photo-reaction of zinc oxide doped with Gadolinium (Gd^{+3}). Around 70 % of acid orange was removed from wastewater using ZnO doped with cadmium oxide (Haghighi and Margan, 2018)

Nano catalysts could be used to degrade organics, remove heavy metals and decompose the pathogens in wastewater and water (Chokshi & Bora, 2014). It could be used in powder form or it could be pre-deposited on the surface of fixed or fluidized absorbers or filters.

Photocatalytic degradation of C.I. Reactive Blue 160 (KE2B) solution using nano ZnO–SnO2 as thin film photocatalyst coated on glass slide showed 60% removal efficacy (Habibi and Mardani, 2015). In the same manner, the ZnO deposited on the surface of porous media achieved 59.25% removal as COD of Textural wastewater.

Chapter Three
Methods and materials

3. Methods and materials

An innovative self-cleaning filtration media was proposed to be synthesized from redundant material like activated carbon or recycled crushed glass. The self-cleaning action was supposed to be achieved by pre-deposition of Zinc oxide (ZnO) nano photocatalysts (NPC) on the surface of the filtration media to degrade the organic matter and other contaminants. Thus, the degradation efficiency of the several types of the synthesized ZnO NPC will be studied in batch experiments as chemical oxygen demand (COD) removal efficiency for secondary effluents of Nablus's western wastewater treatment plant. ZnO NPC could be in the batch experiments as powder or pre-deposited catalyst on the surface of the produced activated carbon or the crushed glass. Figure 3.1 describes the methodology adopted in this research.

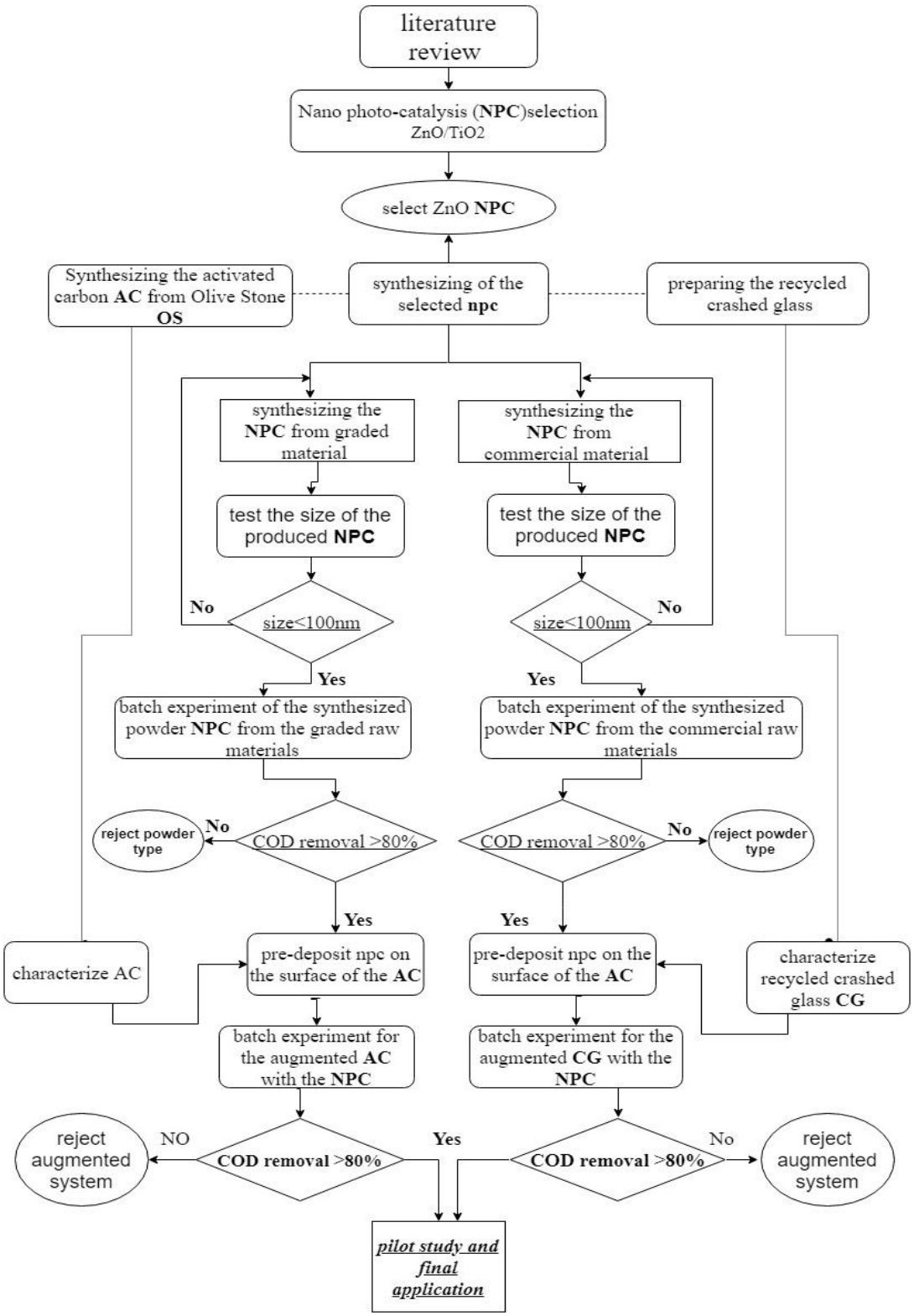


Figure 3.1: Adopted methodology

3.1. Synthesis of activated carbon (AC) from olive stone (OP)

The activated carbon was produced in the lab from the olive pomace OP which was collected from local olive stone presses. First, the raw OP was washed with clean water to remove the pulp, oil, and other dirt that could be attached to the olive seed during and after the olive oil extraction process. The washed olive pomace was sieved then it was dried at 105 C˚. The dried OP was soaked in hexane 95 % to extract the oil from the solid olive pomace. The mixture was heated in water path to the temperature of 45 C˚±2˚ C for 2 h; then, the OP was separated and the hexane was collected to be reused later where the used hexane could be used four more times before oil recovery process using toluene evaporation (EL-Hamouz et al., 2007) see figure(3.2). Then OP was soaked in zinc chloride solution (20% w/w) at room temperature for one day. After that soaking was carried out at 70 C˚ in water bath until evaporating excess water before filter the sample (Zyoud et al., 2015). Filtered OP was heated in tube furnace at 450 C˚ under N_2 gas flow to produce activated carbon AC.

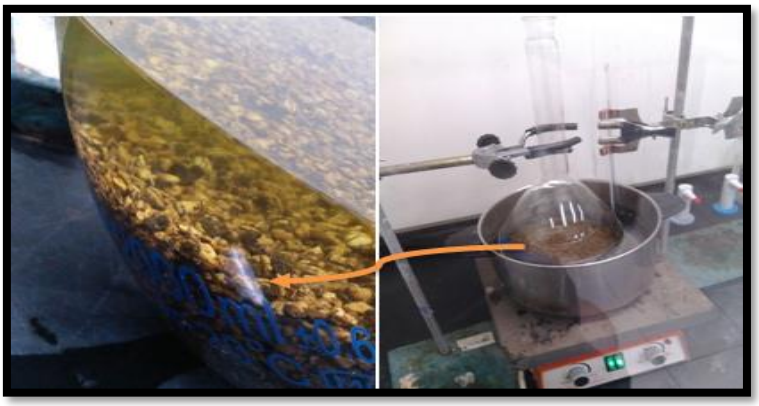


Figure 3.2: Soaking of olive stone in hexane

The produced AC was rinsed with diluted hydrochloric acid, hot deionized water (DW) and cold DW thoroughly. Finally, the produced AC was dried at 110 C˚ and kept to cool in desiccator before storing it in well closed clean container. Figure (3.3) shows the used tube furnace and the produced AC.



Figure 3.3: the used tube furnace and the produced activated carbon

3.2. Characterization of the produced activated carbon AC

3.2.1 Particle size distribution

The produced AC was characterized for size distribution using the ASTM D2862-97 standard test method (ASTM 2010) for Activated carbon classification. The particle size distribution is quit important since it plays a key role in calculating the clean bed head loss for the filtration media. In addition; the smallest size of filtration media grains controls the back wash rate, the wash troughs and gullet heights (Tchobanoglous et al., 2012).

3.2.2. Uniformity coefficient (U) and effective size (D10)

Uniformity coefficient and effective size was calculated after conducting grain size distribution standard test which include plotting the cumulative percentage of the particle size versus the size of the sieve opening in mm. Effective size was defined by reading the sieve opening in mm corresponding to 10 % passing value point at the constructed curve. Then the size in mm corresponding to 60% value (D60) on the constructed curve was defined and divided by the effective size coefficient in mm to get the uniformity coefficient (U) (ASTM 2010).

3.2.3. Specific gravity SG

SG of the produced AC was measured in triple using C 135 - 96 ASTM standard test (ASTM 2003) for true SG of refractory materials by water immersion.

A representative sample of the produced granular AC was taken after mixing the pre-produced AC. A dry pycnometer was filled with distilled water DW and the weight of the stoppered pycnometer was taken before and after DW filling, where the empty dry stoppered pycnometer denoted by **P** and the water-full pycnometer weight denoted by **W1**. Then the pycnometer was dried again at 105˚ C before filling with 1.5 ml of AC sample, the dry stoppered pycnometer and sample was weight **W**. After that, the pycnometer was filled to the half with DW then it was boiled for 15-20 min with gentle swirling to remove all air in the AC porosity. Then it was filled to the mark with cold DW to be weight when it reaches the

room temperature **W2**. Specific gravity SG was calculated using the next equation:

$$SG = \frac{(W - P)}{[(W1 - P) - (W2 - W)]}$$

Where:

p = weight of the stoppered pycnometer (gm)

W = weight of the stoppered pycnometer and sample (gm)

W1= weight of the stoppered pycnometer filled with water (gm)

W2= weight of the stoppered pycnometer, sample, and water (gm)

The SG test was done at room temperature and not varies more than 0.3˚ C during the test. The true SG is the average of the three tests with standard deviation not more than ±3%.

3.2.4. Iodine adsorption number

The Iodine adsorption capacity for the produced AC was tested using D 4607 ASTM standard test method based on three-point adsorption isotherm, where three different weights of the produced AC were treated with standardized iodine solution under specific conditions. After that, the carbon was filtered, see figure 3.4.



Figure 3.4: Filtration of the Iodine solution.

The residual iodine solution was titrated with sodium thiosulfate solution in presence of starch indicator to find the residual iodine normal concentration in the filtrate. The normality of iodine in the residual filtrate was plotted versus the filtrate iodine (X) mg divided by mass of AC samples (M) g, from the constructed graph the iodine number is the X/M corresponding to the 0.02 N iodine concentration in the filtrate. See figure (3.5)

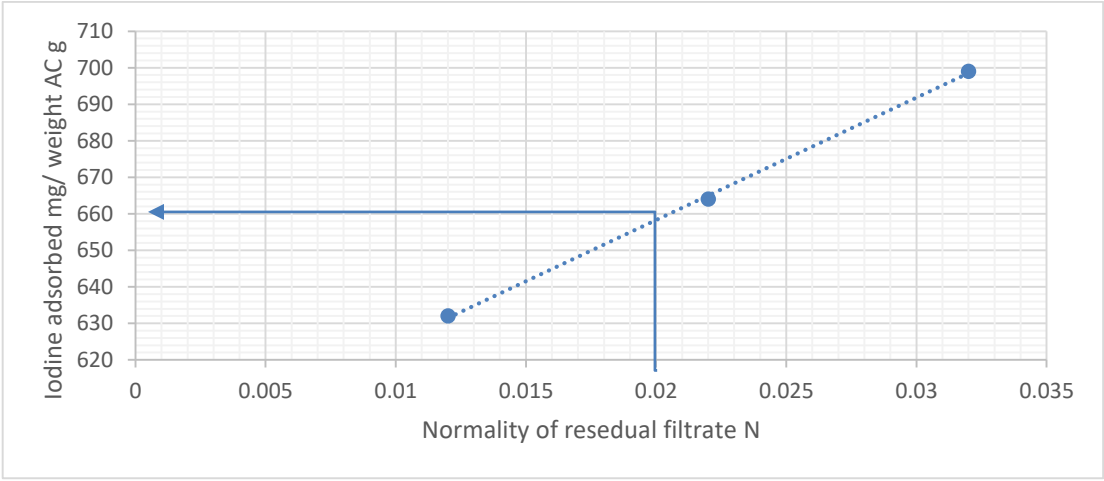


Figure 3.5: Illustration diagram for iodine number

Mianowski et al. (2007) conclude that for the AC with iodine number (IN) in the range of (200-850 mg I_2/g AC) the value of BET surface area and the value of iN are almost the same. The next equation shows the relationship between BET surface area and IN:

$$S_{BET} = 0.986\, IN \cong IN \quad ; 200 < IN < 850\, mg\, I_2\, /g\, AC$$

3.2.5. Surface area using acetic acid adsorption

Specific surface area of the produced AC was determined using Shoemaker and Garland linear Langmuir monolayer adsorption isotherm method (Garland et al., 2009), where the relation between the surface area and the acetic acid monolayer adsorption is described by the next equation:

$$A = \mathrm{N}_m N_a \ \sigma \times 10^{-20}$$

Where,

A= surface area m^2/ g AC.

N_m = slope of the best fit line for the points of (C/N) vs. C.

C= residual acetic acid concentration after titration with NaOH.

N= the number of moles of acid adsorbed per gram of charcoal.

N_a = Avogadro's number = 6.022×10^{23}.

σ= surface area of the acetic acid molecule = 21 $Å^2$.

Six different molar concentrations of acetic acid were prepared (0.3, 0.27, 0.24, 0.21, 0.18 and 0.15 M), then 1 gm samples of AC was added and soaked in volumetric flasks with the prepared acetic acid solutions for 30

min in the mechanical shaker at 125 rpm at room temperature. After that, the samples were kept for 20 min before filtration to reach the equilibrium. The filtrates were titrated with standardized NaOH with phenolphthalein as indicator. The residual acetic acid concentration in each sample was calculated then the adsorbed concentration C_{max} of acetic acid was calculated by subtracting the residual concentration C_t from the original concentration C_0. Then, the number of moles of acetic acid adsorbed per gram of AC was computed (N). N_m in the previous equation is equal to the slope of the best straight line through the points of (C_{max} /N) vs. $C_{max.}$

3.3. Synthesis of zinc oxide (ZnO) nano photo catalyst (NPC)

ZnO nano photocatalyst (NPC) in this research was produced according to two methods. These methods differ in the starting materials purity and composition but the ZnO NPC was produced in the three methods depend on the same chemo-physical production process of simple precipitation. The materials and methods of synthesis are described:

3.3.1. Synthesis of ZnO NPC from graded materials

The ZnO NPC was produced from graded materials. The materials were used as received without any treatment, the methods of synthesis are described below.

A. synthesis ZnO NPC from graded zinc sulfate heptahydrate (ZSH).

ZnO NPC was prepared from zinc sulfate heptahydrate received from Sigma Aldrich ® using precipitation method. The aqueous solution of sodium hydroxide was added slowly to the ZSH aqueous solution in a molar concentration ratio of (1 ZSH: 2 NaOH) under vigorous stirring. And the produced white mortar was stirred for 12 h. After that the mix was left for 1 h before filtering the white precipitate to be washed with DW three times at least. The washed precipitate was dried in oven at 105˚ C and then ground to fine powder using agate mortar see Figure (3.6). The produced white powder is Zn (OH) $_2$ powder. The last step in synthesis of ZnO NPC is heating at 300˚ C (Kumar et al. 2013) for the purpose of dehydroxylation. The synthesized ZnO NPC was kept in clean dark containers.



Figure 3.6: Grinding the precipitate precursor to fine powder using agate mortar and pestle

B. synthesis ZnO NPC from graded micro-sized zinc oxide (μ-ZnO).

Pure micro-size zinc oxide powder (μ -ZnO) was graciously received from Al-Shams Company in Nablus-Palestine as donation. μ -ZnO was added into Ammonium hydrocarbonate solution (80% w/v) in ratio of (under vigorous stirring at room temperature in two steps where third of ZnO was added and stirred until complete dissolving then the rest of ZnO powder was added to the previous solution and stirred for 2 h. In this step urea was added as anti-aggregate agent (Khoshhesab et al. 2012). The resulting white precipitate was dried at 80° C then it were grinded to fine powder using agate mortar and pestle before calcination at 350° C for 2 h.

3.3.2. Synthesis of ZnO NPC from commercial materials

The same procedures in 4.3.1.A and 4.3.1.B were followed to produce the ZnO NPC but using commercial materials. The only modification to the received commercial ZSH and μ -ZnO was the grinding of the row material before synthesis of the ZnO NPC using the mentioned method.

3.4. Ability of synthesized zinc oxide nano photo catalysts naked and supported powder in treating secondary wastewater

The efficiency of produced ZnO powder was tested in experimental batch setup. Where, secondary wastewater (SWW) was brought from western Nablus wastewater treatment plant (WWTP). A beaker of 250 ml was filled out with 150 ml of the SWW and installed in the assembled setup, figure (3.7) illustrate the constructed set up and its' parts. The NPC powder was added and stirred for 10 min to reach equilibrium. Then, the

UV-lamp was turned on and chemical oxygen demand (COD) samples were taken while the SWW sample and the ZnO NPC mixture were stirred vigorously.

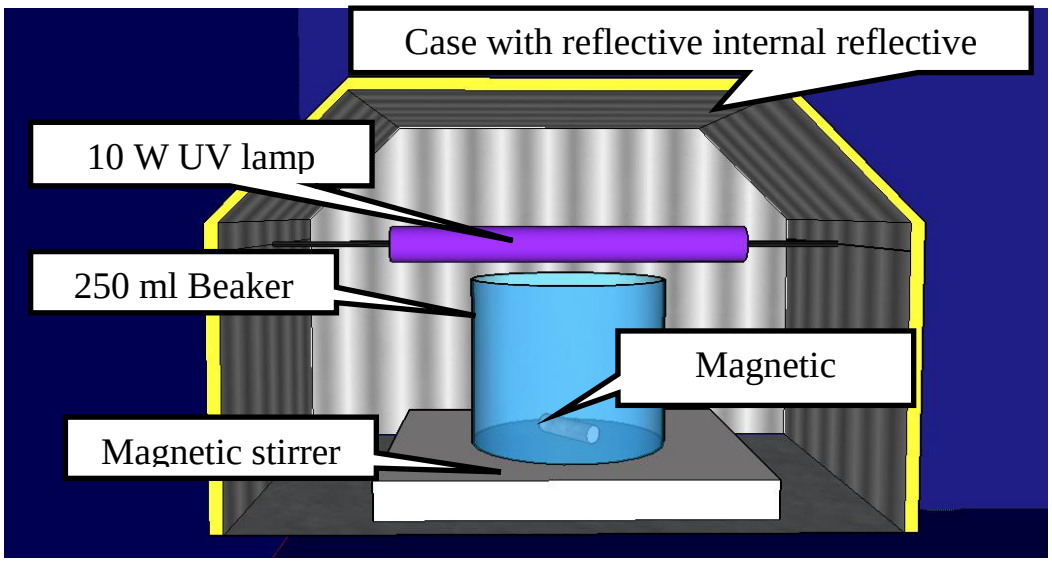


Figure 3.7: Sketch for the designed batch reactor

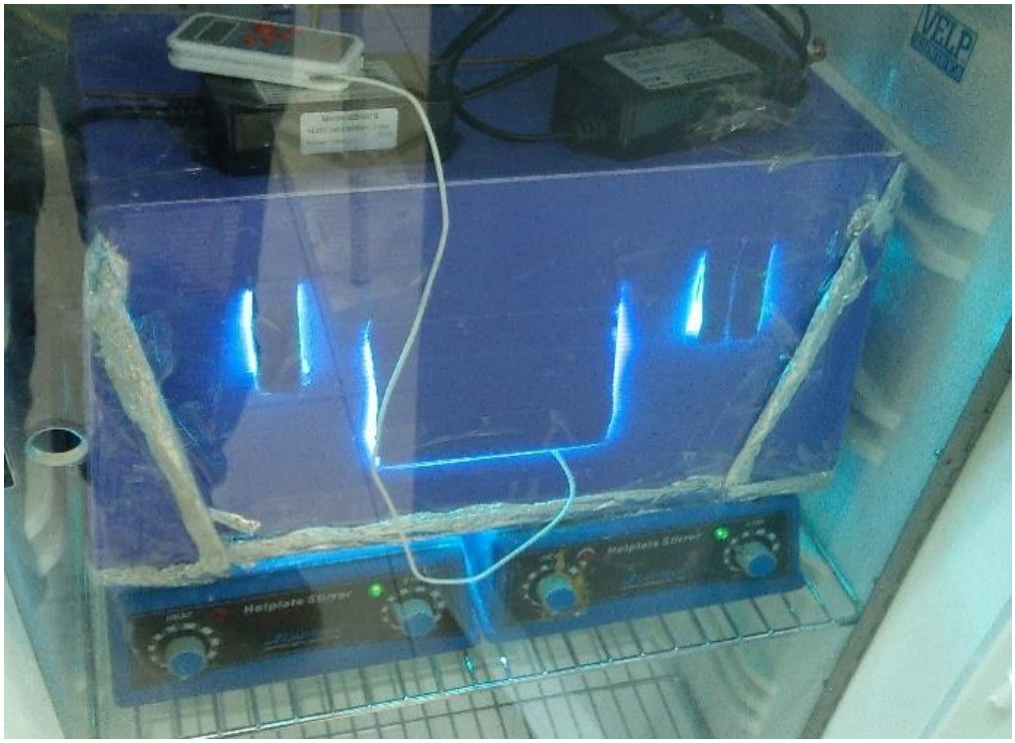


Figure 3.8: Constructed batch reactor containing two batches running simultaneously.

3.4. Chemical Oxygen Demand (COD) testing method

The chemical oxygen demand indirectly indicates the organic pollutants. It is expressed in mg oxygen per litter that is required for oxidizing the organic contaminants in the WW using strong oxidizing agent like potassium dichromate $Cr_2O_7^{2-}$ in presence of silver catalyst. The ASTM- D1252-B (ASTM, 2006) standard test method was used to determine the COD of the collected samples before and after treating with nano photocatalysts. 2 ml of sample were added to the standard low range COD vial of HACH ® Company. After that, the vial was mixed for 10 min and then it was installed in block heater for 2 h at 150˚ C .The absorption of each sample was tested using Thermo ® spectrophotometer device in the Chemical Engineering Department at An-Najah National University, see figure (3.9).



Figure 3.9: The used UV-vis. Spectro-photometer

The standard COD curve was prepared by testing the absorption for three standard solution of potassium hydrogen phthalate KHP with concentration of 425 mg/L which has theoretical COD of 500 mg/L. the next equation describes the reaction (APHA, 2005). Where, seven and half molecules of oxygen consume one molecule of KHP.

$$KC_8H_5O_4 + 7.5O_2 \rightarrow 8CO_2 + 2H_2O + KOH$$

3.5. Pre-depositing of synthesized Nano materials on the surface of the AC filtration media

To overcome the problems of backwashing the filtration media, which is traditionally important to remove the pollutants that block its pores, it was proposed to pre-deposit the ZnO NPC on the surface of the produced AC which could be activated by UV or solar light to degrade these pollutants. This can achieve sustainable and practical solution for the inseparable problem of the persistent backwash. Two graduate researchers at An-Najah National University Ghazi Al-Nour (Ghazi, 2009) and Hussam Amer (Amer, 2012) studied the method of pre-depositing of ZnO NPC at the surface of the activated carbon in order to degrade organic dyes. The pre-deposition method is simple where the ZnO NPC and AC weight ratio of 5:1 mixed in aqueous solution for 40 min with heating to evaporate excess water, see Figure 3.10.

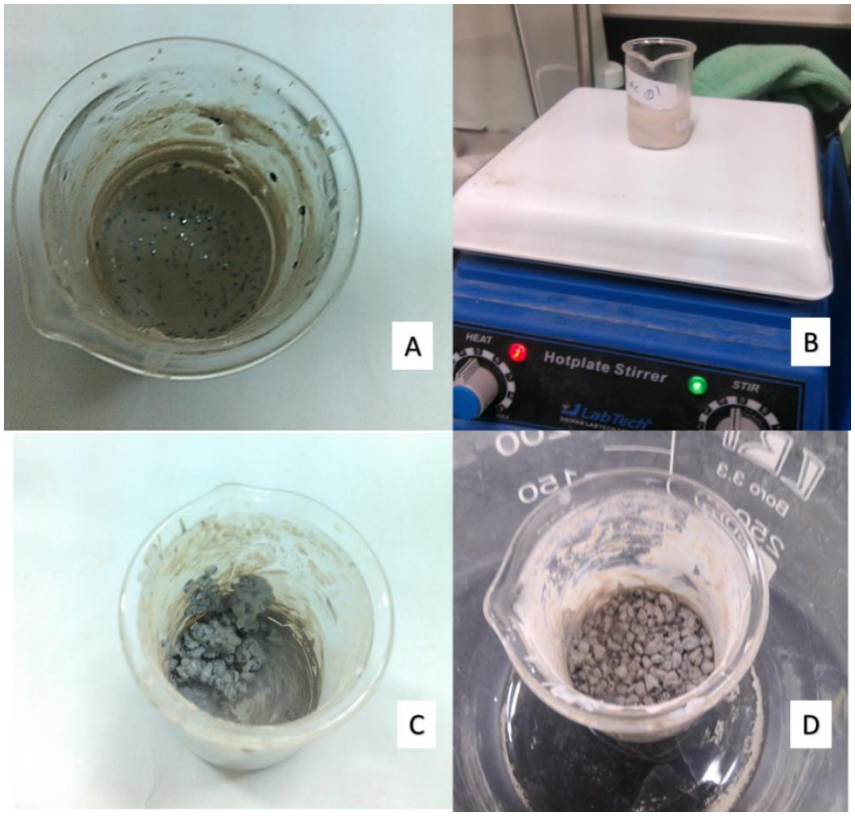


Figure 3.10: Pre-depositing processes of nano ZnO on the surface of the synthesized AC, A) AC and nano zinc oxide wet mixture, B) Mixing on hot plate, C) Dry slurry before calcination, D) Final calcined AC/NPC particles.

3.6. Pre-depositing of synthesized Nano materials on the surface of crushed glass (CG)

The Activated carbon augmented with NPC was found to be not professionally fit to the final application requirements. In addition; the tendency of the black AC to adsorb most of the light that is required for the activation of the photo-catalytic reaction is another reason to search for another filtration media that could fit the required filter specifications. This will be discussed in detail in the Result and Discussion Chapter.

Glass was tested as filtration media and it achieved satisfactory removal efficiency. In this research a development of the glass filtration medias was conducted by thermal augmentation of the NPC on the surface of the glass filtration media. The thermal pre-deposition was done by two methods. The first one is by heating the pre-cleaned crushed bottle glass with the previously prepared ZnO NPC and heated for 30 minutes at the glass softening temperature (550˚-620˚ C). The second proposed method is formation of the zinc hydroxide on the surface of crushed glass by adding the pre-cleaned crushed bottle glass to the aqueous solution of zinc sulfate (see section 4.3.1 A) before titration with sodium hydroxide then it was heated at calcination temperature of 300 C for 2 h for the dehydroxylation, and before cooling it was entered in consecutive cycle of heating to reach the glass softening temperature to achieve the thermal NPC pre-deposition, see figure (3.11).

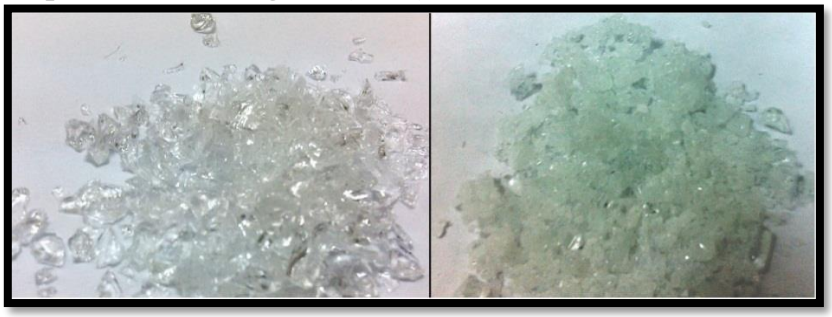


Figure 3.11: The innovated glass filtration media, before and after pre-depositing the NPC

3.7. Scanning electron microscopy test (SEM)

Extra information about the particle size, particles distribution and particle shape were obtained by the SEM test. This test was conducted in

the Institute of Nano Technology at the Jordan University of Science and Technology under the appreciated supervision of Dr. Mohamed Ghazi Al-Fandi. Quanta FEG 450 scanning electron microscope was used to test the powder samples of zinc oxide after fixing it on carbon film, see Figure 3.12.

SEM images were used to compute the particle size using ImageJ 1.X ® software (Schneider et al., 2012).



Figure 3.12: The used SEM.

3.8. X-ray diffraction test (XRD)

The prepared powders were tested with the X-ray diffraction using a Rigaku-Miniflex 600 instrument (see figure 3.13) under the appreciated supervision of Prof. Atef Qusrawi in the Physics Department at the Arab American University- Jenin.



Figure 3.13: Rigaku-Miniflex 600 XRD diffractometer

Powdered samples were kept in dry dark containers and just opened prior the XRD test. A clean piece of glass was dried then painted with glue before application of the NPC powder, see figure 3.14.

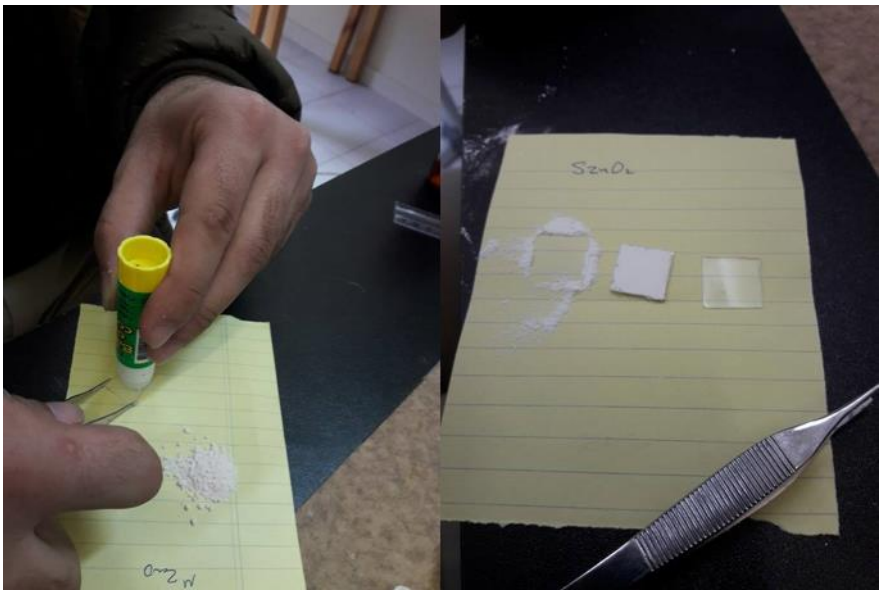


Figure 3.14: Preparing the NPC sample for the XRD test

The particle size of the produced powder was calculated using Debye-Scherrer formula.

$$\text{Particle Size} = \frac{0.9 * \lambda}{\beta \cos\ (\theta)}$$

λ= X-Ray wavelength (0.15405 nm for the used Cu K-alpha X-ray radiation).

β= line broadening at half the maximum intensity.

ϴ= (Bragg's angle in degree) half of the angle corresponding to the maximum intensity.

Chapter Four
Results and discussion

4.1. Characterization of the produced Activated carbon

Activated carbon was produced from olive stone, the pre-cleaned olive stone was soaked in Zinc chloride solution before activation at 450 C˚. The produced AC was characterized for particles size distribution, uniformity coefficient, specific gravity, iodine number and surface area.

4.1.1. Particles size distribution and uniformity coefficient

The size distribution curve shown below indicates that the activated olive stone is well distributed. The effective size (D10) of the AC sample could be determined by obtaining the sieve's size corresponding to the 10% finer on the cumulative finer curve which equal to 0.3 mm, and the size at which the 60% of the sample finer than it (D60) is 2.0 mm thus the uniformity coefficient equal to D60/D10 and equal to 6.7.

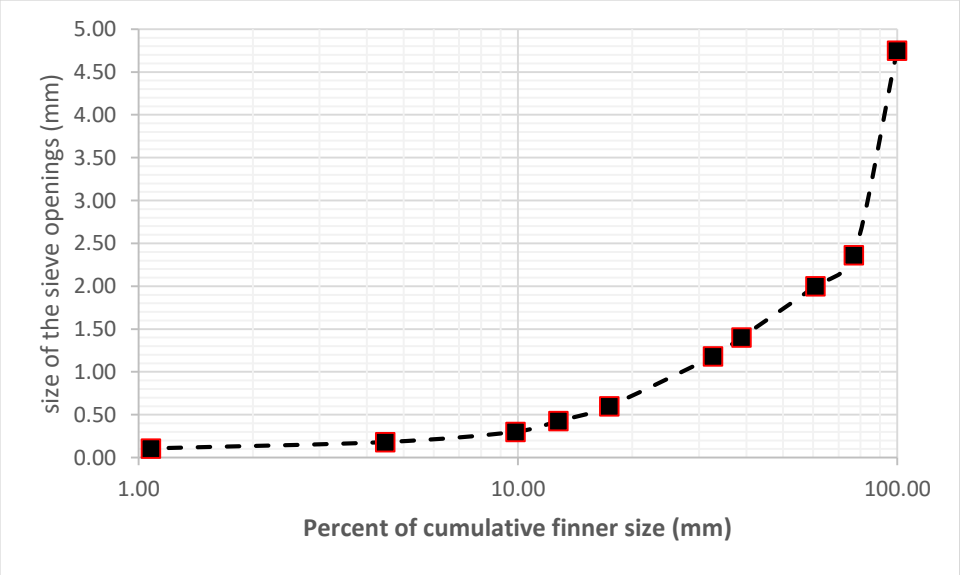


Figure 4.1: Particle size distribution for the produced AC

The produced activated carbon contained a lot of fine material with size less than the minimum effective size of 0.8 mm according to the granular activated carbon's filters-specifications (see section 3.1).

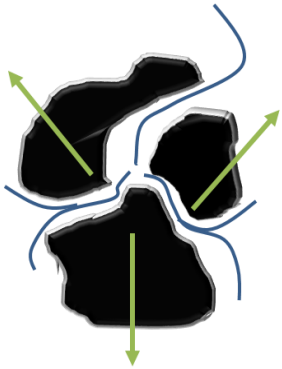
It was expected for such filtration media of the previous size distribution (including all fine grains) to develop high head loss during filtration of the secondary waste water. Indeed, this may be true in sand, ilmenite and anthracite filtration medias, but it doesn't develop the same high head loss in the produced AC filtration media. In fact, the real dynamic head loss doesn't exceed 5 cm while the theoretical one overrides four meters.

The explanation for this incompatibility between the real and theoretical head loss is that, all head loss formulae neglect the density of the filtration media which could be significant in loose light media. The produced AC has a SG of 0.76 ± kg/l that makes it light enough to be slightly budge allowing the gravitational flow to go down without mass obstruction or retardation.

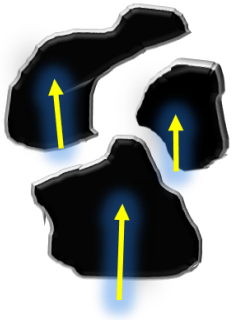
4.1.2. Specific gravity (SG)

Specific gravity of the produced AC was tested in triplicate and it was found to equal 0.76 ± .026. This SG is significantly less than the recommended specifications for gravity filters which is from 1.5 to 1.8 (EPA, 1995) [see section 3.1]. However, the low specific gravity for the activated carbon grains in the filtration media facilitate the movement of the down flow through the filtration media see figure (4.2). Indeed, two

dominant forces affect the loose filtration media grains and could cause slight movement to the AC grains.



Dynamic force reposition the light carbon media's grains



Buoyancy force slightly shift the light carbon media's grains

Figure 4.2: Forces that affect the filtration media and cause slight movement to its grains

4.1.3. Surface area

Surface area was tested using acetic acid adsorption according to Langmuir monolayer adsorption isotherm (see the next equations)

$$\frac{C_e}{N} = \frac{C_e}{N_m} + \frac{1}{\mathrm{k} * N_m}$$

$$\frac{C_e}{\mathrm{N}} = \frac{\mathrm{k} * C_e + 1}{\mathrm{k} * N_m}$$

$$\text{Surface area } (SA)\ m^{\,2} = N_m N_A \sigma * 10^{-20}$$

Ce = equilibrium solute concentration.
N= number of moles adsorbed per gram of AC.
Nm= the number of moles per gram AC required to form monolayer.

K= constant (function of temperature).

N_A= Avogadro's number.

σ= surface area of one acetic acid molecule in square angstrom.

Slope of the best fit line in Figure 4.3 equal to 794.22 g/mol and equal to 1/Nm thus the moles of acetic acid adsorbed per gram of activated carbon (Nm) equal to 1.26×10^{-3} mole/g. the surface area of acetic acid molecule is 21 $Å^2$. Thus the produced AC has a surface equals the number of adsorbed moles multiplied by Avogadro's number multiplied by the surface are of acetic acid molecule and equal to 159.22 m^2 / gm.

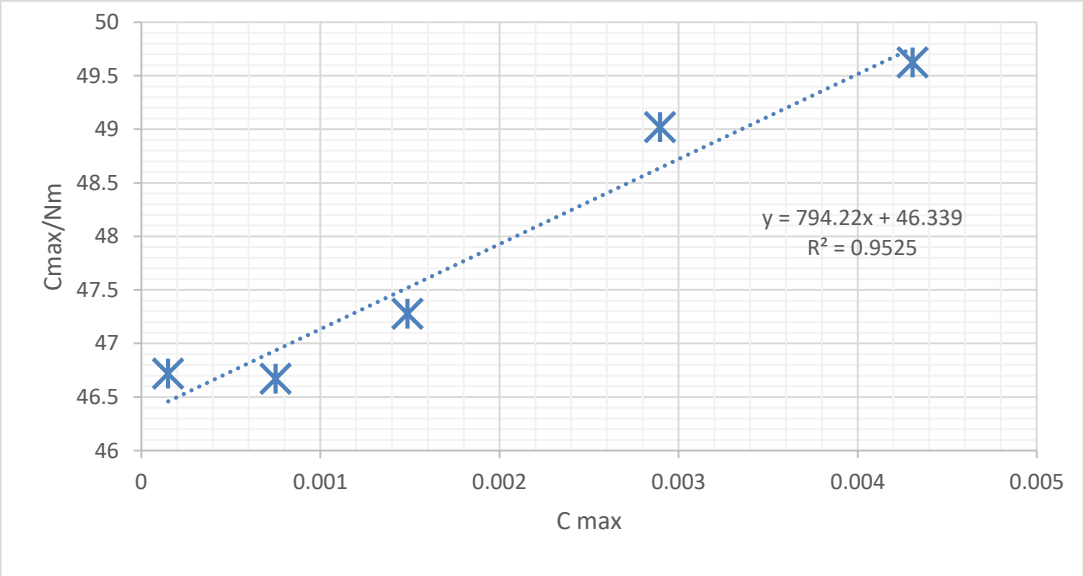


Figure 4.3: Plot of C_{max} vs. C_{max}/N_m.

4.1.4. Iodine number (IN)

Iodine adsorption isotherm was used to determine the relative activation level of the produced activated carbon. Where, the IN is reported as the amount of iodine adsorbed in milligrams per gram of AC at residual iodine concentration of 0.02 N. from the iodine adsorption isotherm in the

next figure iodine number is equal to the milligrams of adsorbed iodine per gram carbon corresponding to the residual concentration of 0.02 mg/l and equal to 166.94 mg/g.

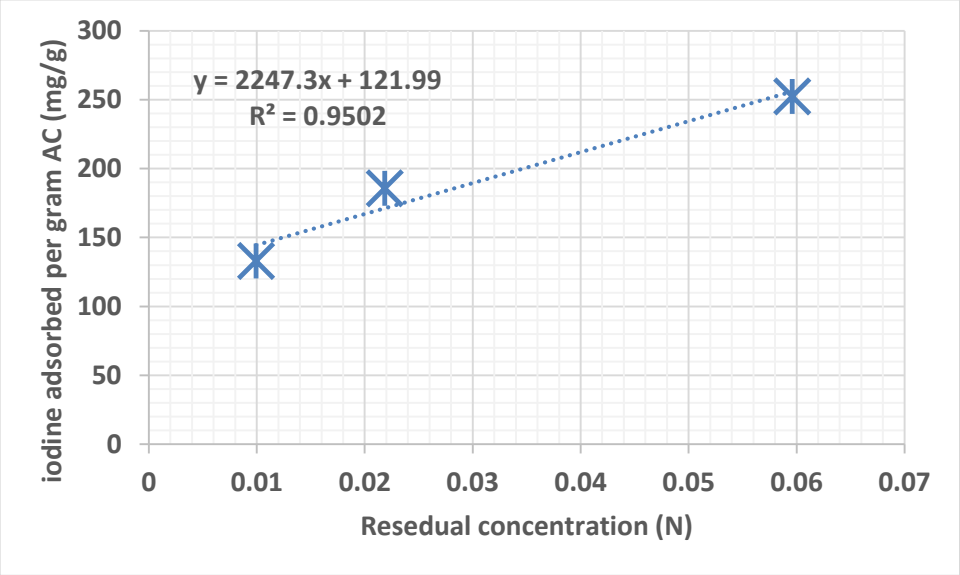


Figure 4.4: Plot of Resedual concentration vs. $C_{max}/N_{m.}$

4.2. SEM - characterization of the produced Zinc oxide nano-catalysts

SEM test was conducted to characterize the size and shape of the produced nano catalysts. All SEM tests were conducted using an accelerating voltage of 30 kV.

4.2.1. Nano zinc oxide produced from zinc sulfate heptahydrate (ZSH)

The zinc oxide nano photo catalysts were produced from commercial and graded zinc sulfate heptahydrate with purities of 95% and 99.5% respectively. Figures 4.5 and 4.6 show the images which were taken for the powder samples by the scanning electron microscope. The shape of

ZnO particles are rod-like in both cases (graded and commercial raw materials) but the ZnO produced from graded materials have an agglomerated rod-like particles with little proportion of flower like particles. By contrast, nano ZnO produced from commercial zinc sulfate heptahydrate produces separate rod-like particles.

Figures 4.7 and 4.8 show the average particle area which was measured using ImageJ ® software. The ZnO nano powder produced from commercial ZSH has an average particle size of 69 nm and the nano powder produced from graded ZSH has an average particle size of 29 nm.

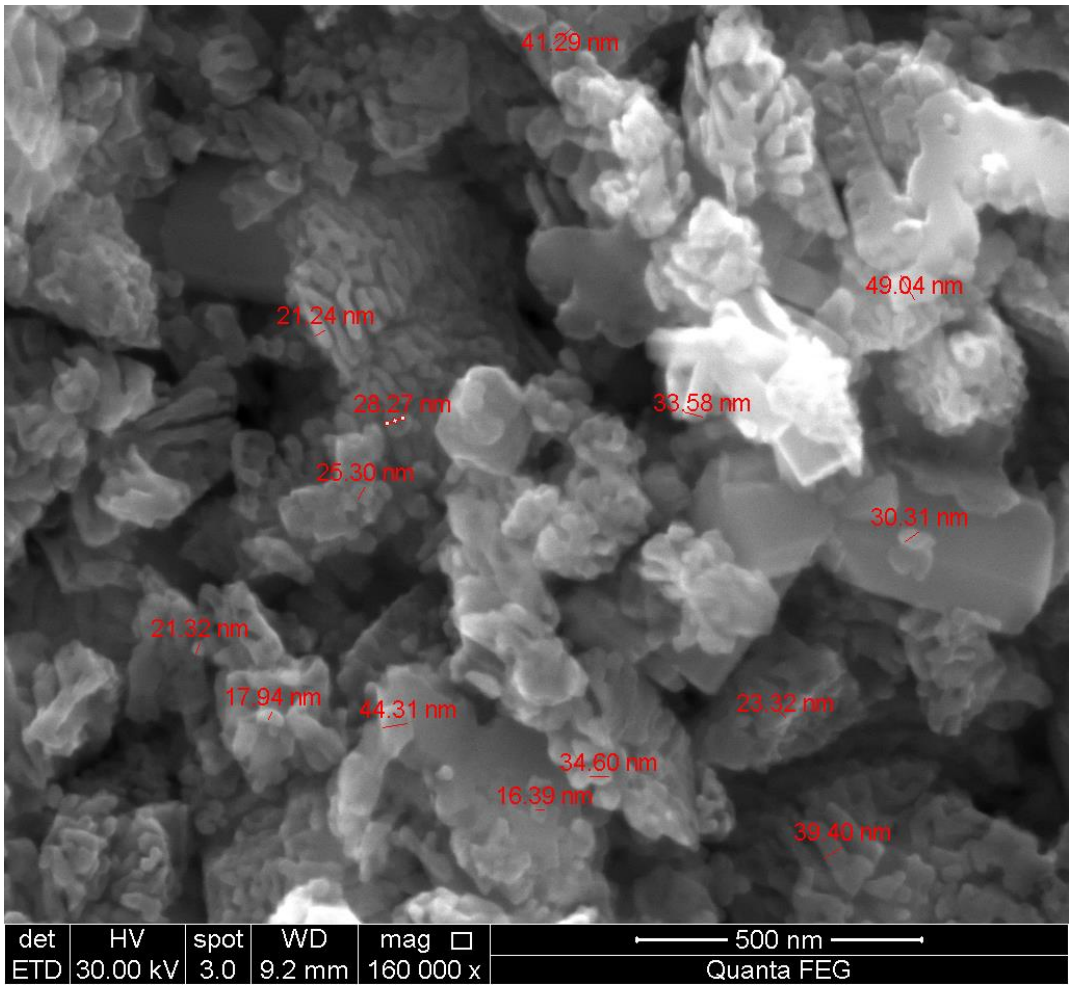


Figure 4.5: Nano catalysts produced from graded quality of zinc sulfate heptahydrate.

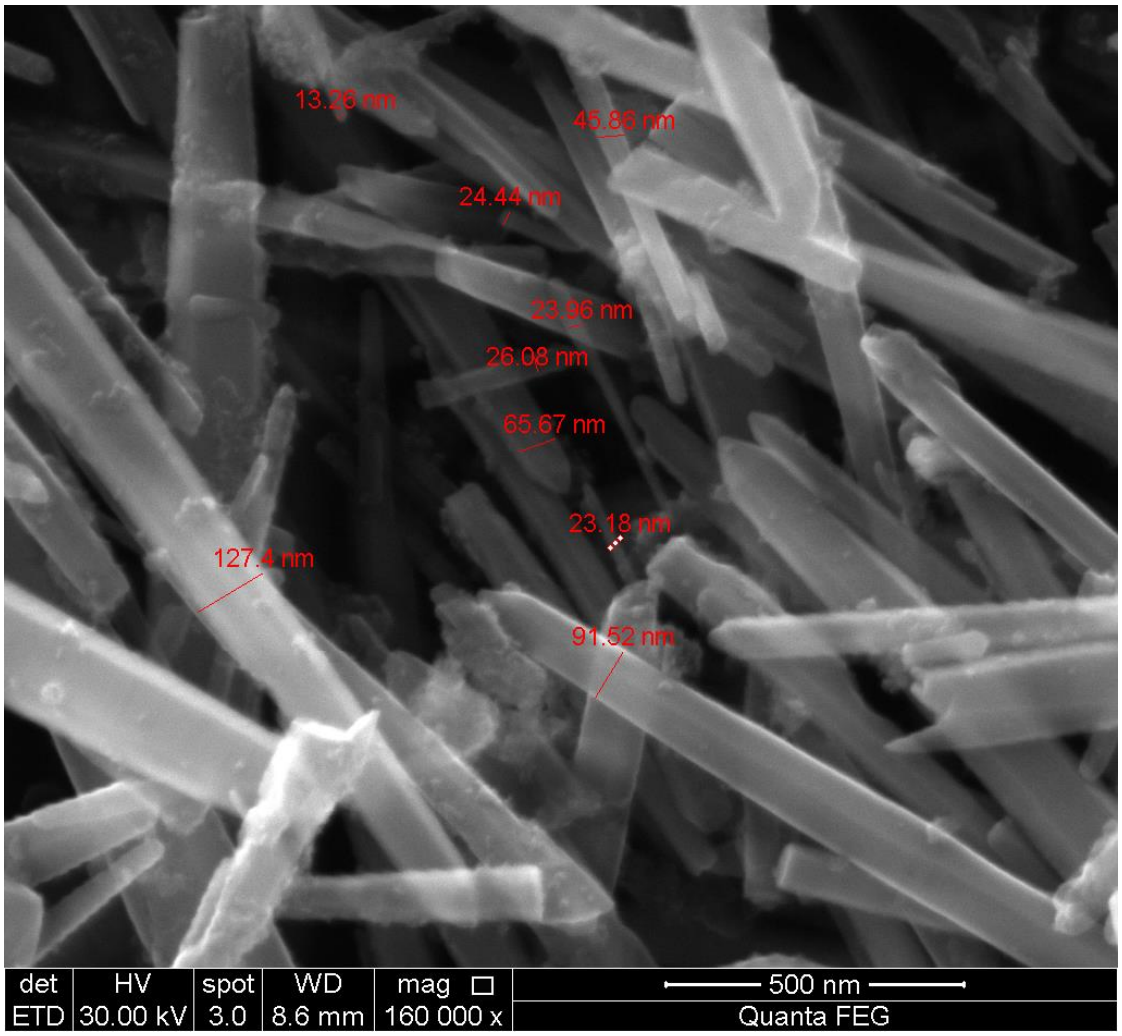


Figure 4.6: Nano catalysts produced from commercial quality of zinc sulfate heptahydrate.

Nano catalysts produced from commercial quality of zinc sulfate heptahydrate

Results

File Edit Font Results **Diameter**

	Label	Area	Mean	Min	Max	Angle	Length
5		65.158	83.4´2	72.588	89.764	51.843	33.404
6		51.440	157.´29	´31.615	184.649	90.000	26.084
7		65.158	79.3´1	62.485	92.160	49.399	33.404
8		48.011	195.449	´72.113	206.742	102.995	24.048
9		48.011	100.507	86.666	105.975	90.000	23.475
10		48.011	97.063	78.064	102.610	61.390	23.330
11		48.011	151.795	´24.223	176.338	57.529	24.607
12		68.587	97.707	87.778	104.157	64.799	34.995
13		78.875	118.083	´06.415	126.680	58.570	39.815
14		65.158	163.´16	´54.449	168.672	122.005	34.009
15		96.022	121.749	´13.859	147.580	96.340	49.833
16		75.446	84.5´0	74.969	89.744	48.814	38.776
17		68.587	57.460	35.992	63.782	15.524	35.478
18		61.728	140.944	´37.625	146.238	6.710	31.732
19		48.011	89.552	68.312	109.337	141.340	24.048
20		58.299	92.493	79.786	103.110	122.735	30.419
21		82.305	94.487	76.237	116.002	95.194	42.059
22		51.440	130.259	´18.567	144.050	111.038	25.690
23		34.294	88.666	80.317	94.864	75.964	16.497
24		41.152	82.778	77.040	85.841	59.036	21.029
25		41.152	68.463	65.189	71.523	90.000	20.867
26		41.152	85.331	81.406	91.865	52.125	20.372
27		54.870	131.967	´04.985	155.026	90.000	28.692
28		54.870	96.520	87.235	104.054	105.945	27.232
29		54.870	96.520	87.235	104.054	105.945	27.232
30		72.016	136.856	´04.680	161.418	92.862	36.610
31	Mean	57.385	111.708	96.170	123.231	74.195	29.138
32	SD	14.824	32.065	29.372	36.024	33.533	7.845
33	Min	34.294	57.460	35.992	63.782	6.710	16.497
34	Max	96.022	195.449	´72.113	206.742	141.340	49.833

Figure 4.7: ImageJ® results for average particle diameter of the nano catalysts produced from graded quality of zinc sulfate heptahydrate.

Nano catalysts produced from commercial quality of zinc sulfate heptahydrate

Results

File Edit Font Results **Diameter**

	Label	Area	Mean	Min	Max	Angle	Length
4		219.479	160.699	84.000	215.689	18.435	117.121
5		147.462	150.620	63.000	199.000	87.274	77.866
6		58.299	132.941	110.000	154.000	90.000	29.630
7		168.038	83.734	34.000	102.667	75.379	88.036
8		106.310	80.278	53.000	96.200	61.699	54.685
9		102.881	117.551	111.082	137.000	74.055	53.927
10		96.022	68.375	59.136	90.111	41.987	49.828
11		270.919	103.882	82.000	165.077	95.856	145.202
12		109.739	88.038	77.094	114.000	39.806	57.854
13		164.609	110.410	89.000	116.362	62.354	87.802
14		75.446	54.961	46.537	63.837	119.055	38.132
15		96.022	45.033	15.959	60.376	53.973	50.376
16		236.626	91.303	53.213	115.829	161.030	125.325
17		168.038	108.498	67.000	122.194	73.072	89.043
18		106.310	71.939	55.422	89.600	47.726	55.060
19		92.593	18.365	8.385	24.000	4.399	48.290
20		181.756	109.312	85.000	117.154	85.601	96.581
21		147.462	136.230	97.000	153.000	64.654	77.866
22		140.604	84.024	25.000	115.000	69.775	74.994
23		140.604	60.981	28.000	84.168	69.775	74.994
24		96.022	73.525	58.852	90.000	41.987	49.828
25		274.348	92.368	16.614	163.000	98.746	146.144
26		78.875	130.696	61.000	148.289	33.690	40.062
27		65.158	46.232	28.000	55.185	63.435	33.127
28		75.446	109.381	94.000	135.211	163.301	38.668
29		102.881	95.560	55.000	132.895	114.775	53.029
30		116.598	52.550	16.000	65.992	-122.735	61.642
31	Mean	131.916	95.056	61.464	118.661	70.212	69.396
32	SD	57.889	35.857	32.768	44.748	52.748	31.410
33	Min	58.299	18.365	8.385	24.000	-122.735	29.630
34	Max	274.348	160.699	147.625	215.689	163.301	146.144

Figure 4.8: ImageJ® results for average particle diameter of the nano catalysts produced from commercial quality of zinc sulfate heptahydrate.

4.2.2. Nano zinc oxide produced from micro-sized zinc oxide (μ-ZnO)

Figure 4.9 shows the SEM result for the ZnO that was produced from commercial purity of μ-ZnO which indicates agglomerated sphere-like particles with average particle size of 28 nm, see Figure 4.10.

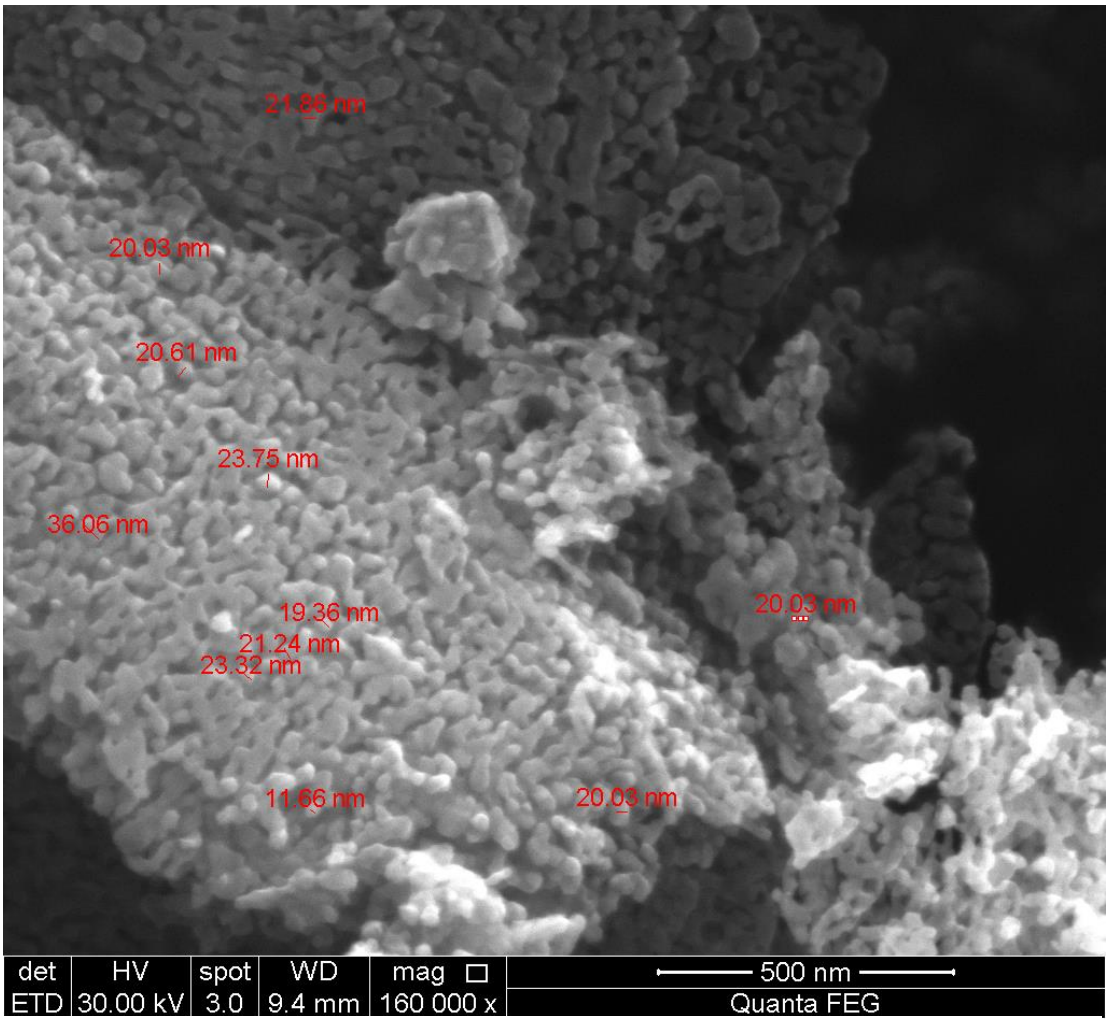


Figure 4.9: Nano ZnO catalysts produced from commercial quality of μ-ZnO.

Nano ZnO catalysts produced from commercial quality of μ-ZnO

Results

File Edit Font Results **Diameter**

	Label	Area	Mean	Min	Max	Angle	Length
5		34.294	216.548	176.028	238.712	139.399	16.702
6		54.870	181.562	156.404	201.037	143.130	28.214
7		48.011	174.013	139.434	212.242	90.000	23.475
8		54.870	177.304	134.835	212.933	90.000	28.692
9		41.152	102.332	81.563	113.527	59.036	21.029
10		48.011	149.580	125.858	167.830	85.236	23.620
11		48.011	159.617	130.420	186.338	38.660	24.048
12		48.011	179.490	146.815	214.070	65.556	23.330
13		106.310	148.150	125.207	162.814	97.853	55.332
14		61.728	150.446	94.616	165.656	93.366	31.409
15		44.582	68.401	63.012	77.423	74.745	21.509
16		34.294	242.613	198.734	254.651	97.125	15.866
17		58.299	169.452	120.376	220.437	71.565	29.740
18		61.728	150.727	114.265	163.014	90.000	31.301
19		48.011	163.562	156.119	171.943	122.471	24.607
20		58.299	151.909	118.914	195.017	63.435	29.163
21		48.011	143.007	106.823	162.757	28.610	23.330
22		58.299	164.074	135.153	183.024	14.036	29.740
23		61.728	116.764	105.054	124.348	132.510	31.409
24		34.294	108.010	92.089	122.807	116.565	17.498
25		72.016	134.030	106.843	151.212	111.251	36.331
26		54.870	147.143	126.950	180.004	66.801	28.093
27		51.440	89.925	75.184	96.972	0.000	26.084
28		58.299	154.219	143.875	162.165	119.745	30.419
29		89.163	60.349	58.448	64.716	104.036	45.553
30		54.870	142.606	87.658	173.217	66.801	28.093
31	Mean	54.984	148.777	122.028	168.518	90.004	27.810
32	SD	16.836	37.679	31.784	43.752	38.931	8.982
33	Min	24.005	60.349	58.448	64.716	0.000	11.665
34	Max	106.310	242.613	198.734	254.651	176.634	55.332

Figure 4.10: ImageJ® results for average particle diameter of the nano catalysts produced from commercial quality of μ-ZnO.

The shape and size of the produced particles are quite different based on the preparation method and purity of the raw materials; Thus, its believed to have different surface area and chemical behavior; For instance, nano catalyst produced from commercial purity of zinc sulfate heptahydrate shows higher stability against reduction under the influence of UV. Moreover, it shows higher degradation ability of the contaminant in the WW, this observations were discussed in section 4.4.

The raw micro zinc oxide was tested using SEM and the results indicate similarity in crystals size and shape for both commercial and graded quality of raw materials: see Figures 4.10 and 4.11. Particle size of the micro ZnO powders was analyzed using the ImageJ ® software and the results indicate convergent particle size for both commercial and graded purity with size around 0.22 μm.

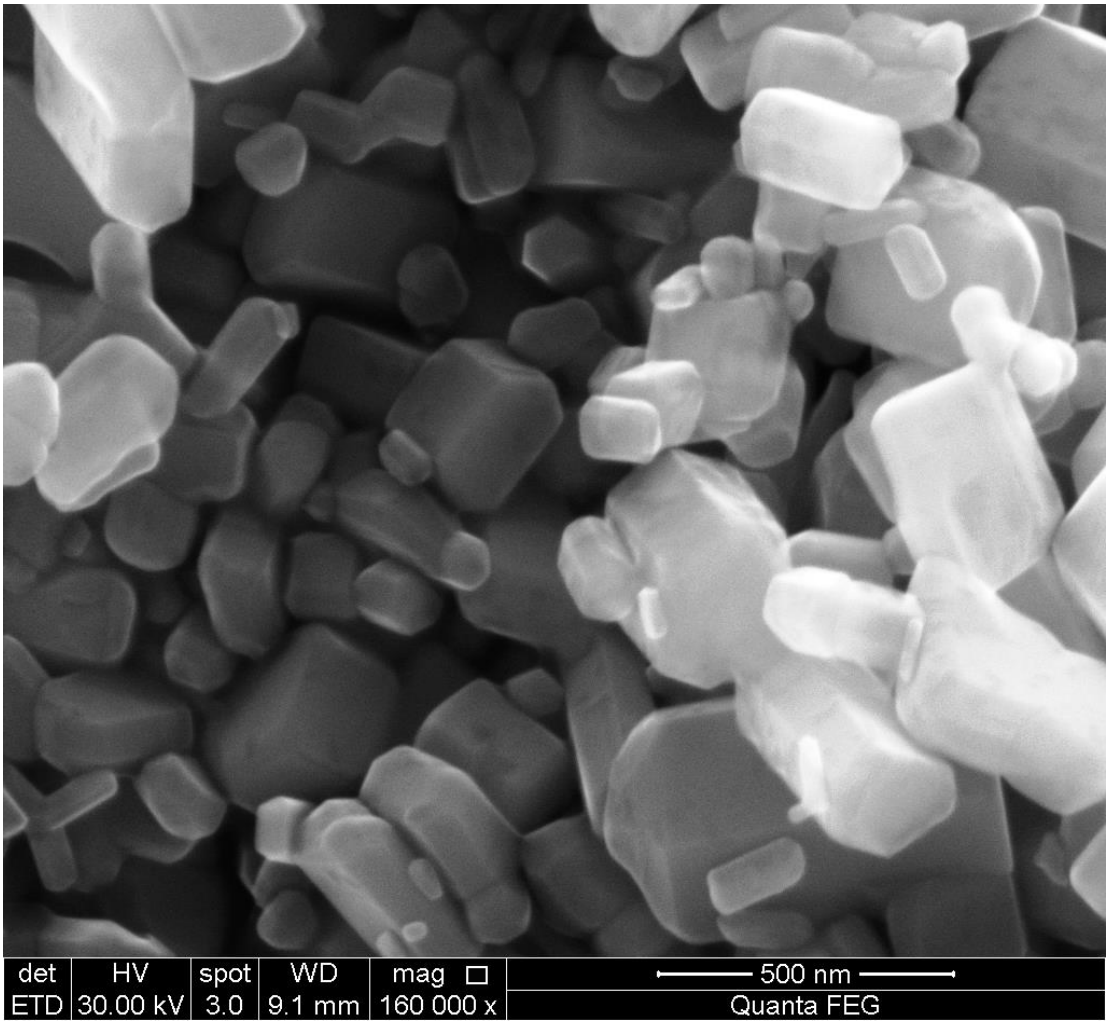


Figure 4.11: Graded quality of micro Zinc Oxide.

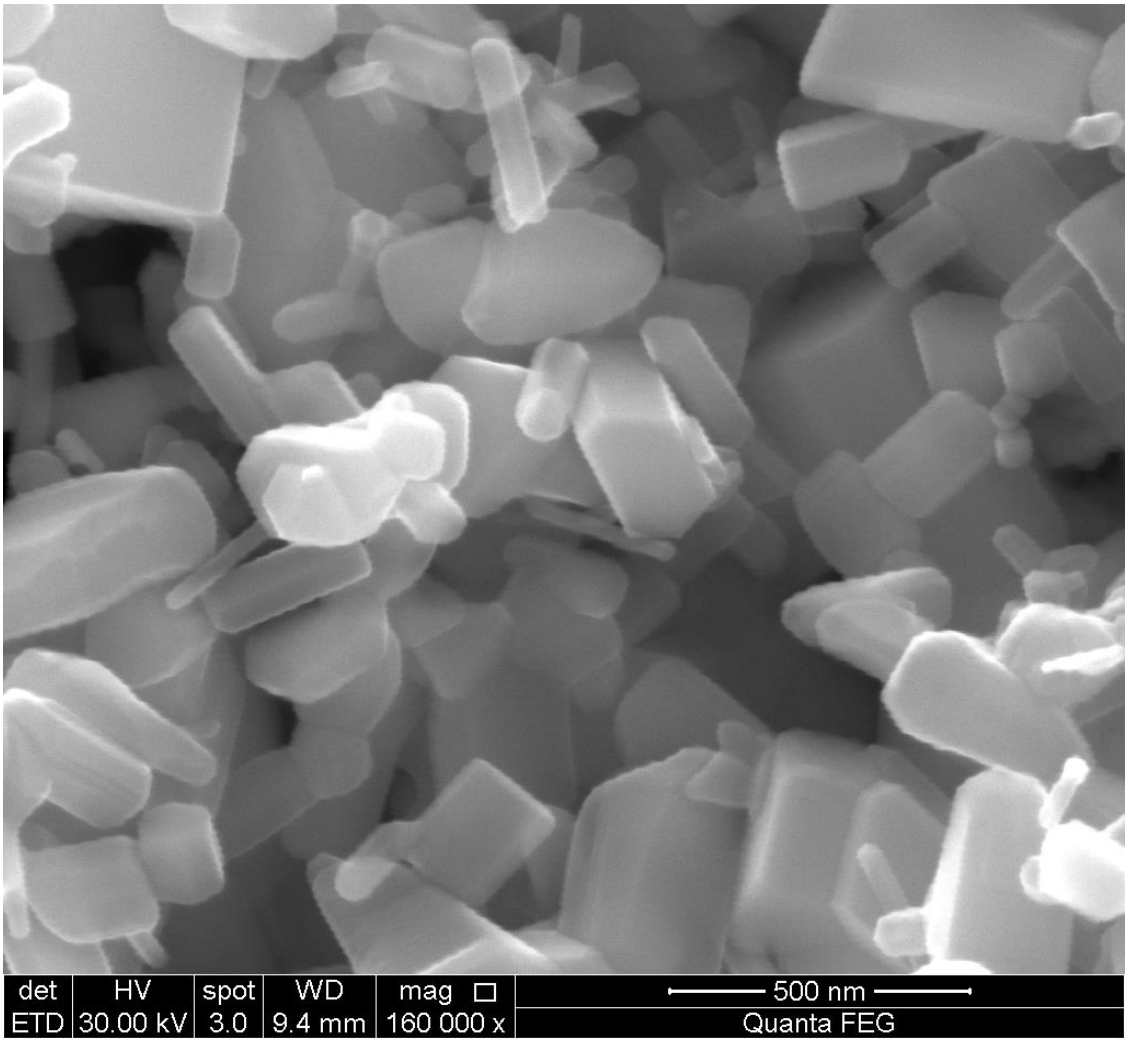


Figure 4.12: Commercial quality of micro Zinc Oxide.

4.3. XRD- characterization of the produced Zinc oxide nano-catalysts

The produced nano zinc oxide catalyst and the raw micro zinc oxide were also characterized for the crystal size by measuring the X-Ray diffraction pattern. The measured pattern was used to calculate the size of nano crystal using Debye-Scherrer formula, which indicates different size than SEM test results what requires finding a correction parameter.

4.3.1. Nano zinc oxide produced from zinc sulfate heptahydrate (ZSH)

XRD test for zinc oxide nano photo catalysis which was produced from commercial and graded zinc sulfate heptahydrate indicates well crystallized materials with sharp diffraction peaks; see the next figures.

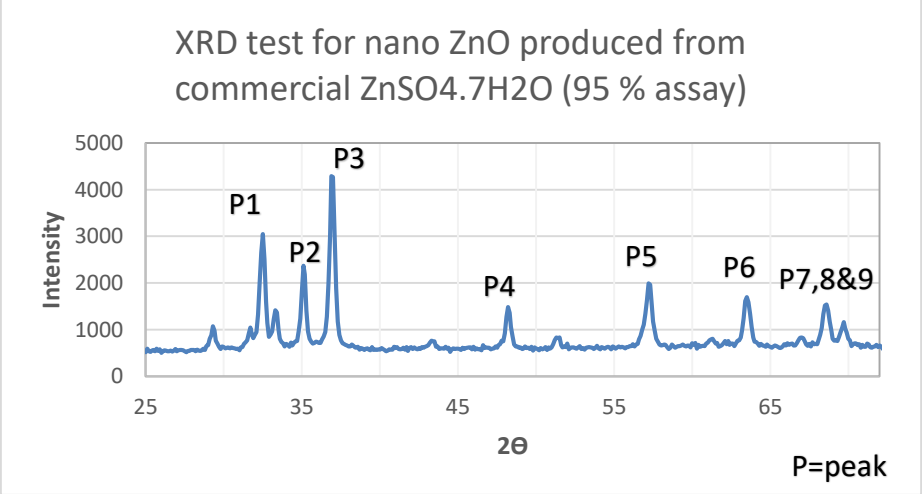


Figure 4.13: X-Ray diffraction pattern for nano ZnO produced from commercial ZnSO4.7H2O

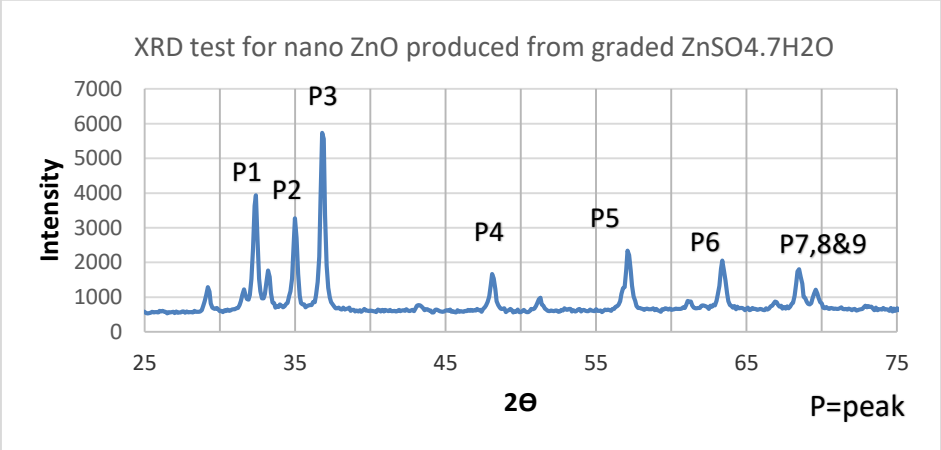


Figure 4.14: X-Ray diffraction pattern for nano ZnO produced from graded ZnSO4.7H2O.

Peaks in the X-ray diffraction patterns of the produced powders fit the peaks on the RRUFF's standard curve of zinc oxide (R060027) with less than 1 degree shift (RRUFF Database, 2015). Figure (4.15) shows the first three X-ray diffraction peaks for both synthesized and standard ZnO.

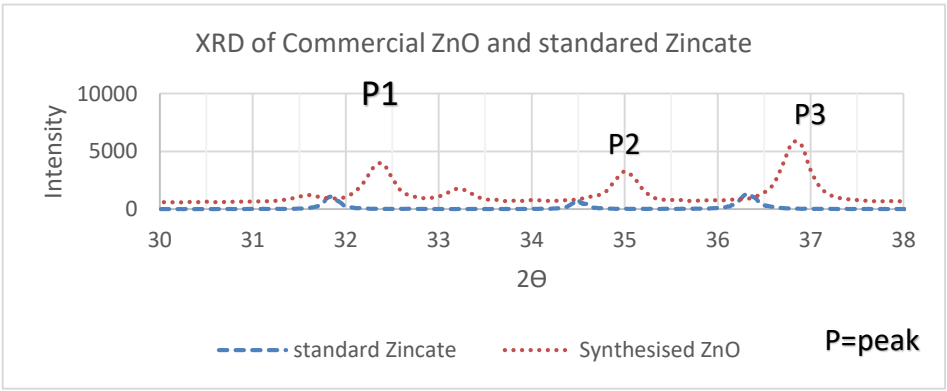


Figure 4.15: Diffraction pattern of X-ray for commercial ZnO and standard Zincate RRUFF ID: R060027.2**.**

Particle size of the produced powders was derived from the XRD curve using Debye-Scherrer equation. The next table shows the diameter of the produced graded and commercial precursor powder particles:

Table 5: Diameter of the produced ZnO (nm) from commercial and graded raw precursor

Peak No. / Powder type		peak1	peak2	peak3	peak4	peak5	peak6	Average Size (nm)
Zinc oxide produced from commercial ZnSO4.7H2O (purity 95%)	2Ɵ	32.5	35.1	36.9	48.2	57.2	63.5	26.5
	D	21.6	29.0	21.9	22.7	31.5	32.5	
Zinc oxide produced from grade ZnSO4.7H2O (purity 99.5%)	2Ɵ	32.4	35.3	37.1	48.4	57.4	63.6	25.7
	D	21.6	29	29.2	18.2	23.6	32.5	

According to the results above the commercial and graded quality of zinc sulfate heptahydrate raw precursor doesn't significantly affect the size of the produced zinc oxide. At the same time, the cost of regent grade raw precursor is ten times more expensive than the commercial one. Thus, using raw materials with commercial quality is more reasonable based on economical consideration, provided that the cost of 1 kg of ZSH with graded high purity (99.5% purity) is 135 US dollar while the cost of the ZSH powder with commercial purity (98% purity) is 18.4 US dollar for one Kg.

4.3.2. Nano zinc oxide produced from micro-sized zinc oxide (μ-ZnO)

Nano zinc oxide catalyst was produced from the graded high purity and commercial micro-sized zinc oxide with purities of 99% and 95% respectively. The produced powders have X-ray diffraction patterns less

sharp than what was observed previously for the nano ZnO synthesized from $ZnSO_4.7H_2O$, especially in the last peaks (P7,P8 and P9). But, it still has a diffraction pattern indicating well crystallized; see the next figures.

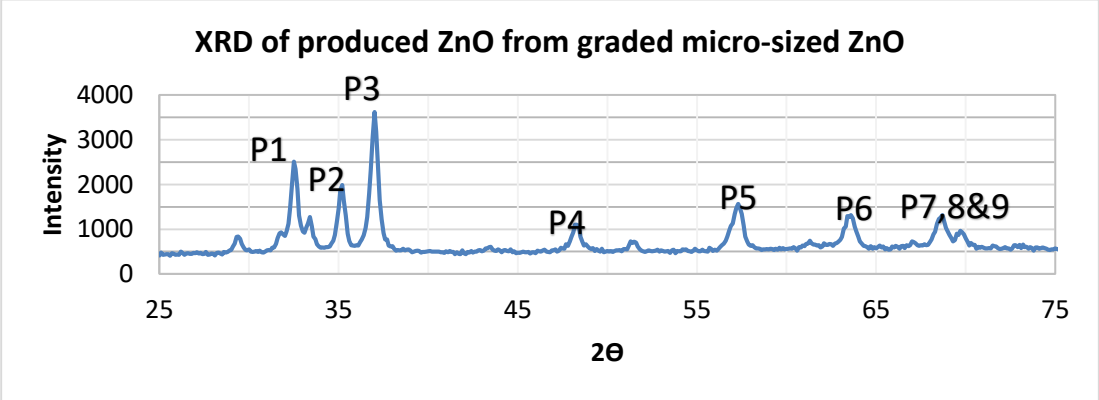


Figure 4.16: XRD pattern of produced ZnO from graded micro-sized ZnO.

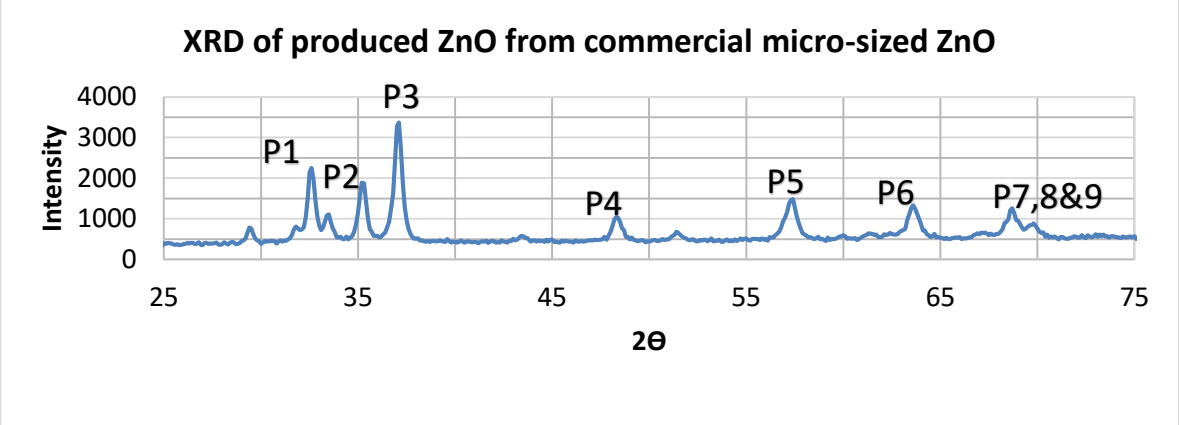


Figure 4.17: XRD pattern of produced ZnO from commercial micro-sized ZnO.

Table 6: properties of the produced nano ZnO from commercial and graded raw micro sized ZnO

		Peak1	*Peak 2*	*Peak 3*	*Peak 4*	*Peak 5*		*Peak 6*	*Average*
*Size of ZnO produced from **µ**ZnO with graded purity*	**$2\Theta_s$**		32.5	35.2	37.0	48.4	57.4	63.7	
	D (nm)		21.6	21.8	17.5	18.2	11.8	10.9	17.0
*Size of ZnO produced from **µ**ZnO with commercial purity*	**$2\Theta_s$**		32.6	35.2	37.0	48.4	57.4	63.7	
	D (nm)		21.6	29.0	21.9	15.2	13.5	10.9	18.7
$2\Theta r$ for the peaks of standard references	**$2\Theta_r$** for the peaks of RRUFF's reference ID: R050419		31.77	34.53	36.24	47.52	56.54	62.81	
	$2\Theta_r$ for the peaks of RRUFF reference ID: R050492		31.75	34.42	36.23	47.51	56.55	62.81	
	$2\Theta_r$ for the peaks of RRUFF reference ID: R060027.2		31.82	34.47	36.3	47.59	56.64	62.91	
Absolute difference between peak's locations of the produced sample and standard sample ($|2\Theta_s - 2\Theta_r|$)	RRUFF ID: R050419		0.8	0.7	0.8	0.9	0.9	0.9	0.82
	RRUFF ID: R050492		0.75	0.78	0.77	0.89	0.85	0.89	0.77
	RRUFF ID: R060027.2		0.68	0.73	0.7	0.81	0.76	0.79	0.70

Compared to the ZnO NPC produced from the $ZnSO_4.7H_2O$, the produced nano ZnO from μ-ZnO has a slightly smaller particle size. Similar to the previously produced nano ZnO, X-ray diffraction pattern for the produced powder from graded and commercial μ-ZnO indicates small shift inpeak positions between reference sampleand synthesized powders. By the same token, the commercial raw precursor is preferable based on economic considerations since there is no significant difference in size between the produced powder from graded and commercial μ-ZnO.

4.4. Photo catalytic degradation ability using different types of synthesized zinc oxide powders

4.4.1. Nano zinc oxide produced from commercial Zinc Sulfate Heptahydrate

Batch experiments were conducted using 0.25 g ZnO catalyst in 100 ml of secondary waste water from Nablus Western Treatment Plant. The experiment was conducted in duplicate simultaneously. Notably, COD of the secondary effluent declined rabidly under the influence of the photo catalytic reactions which was activated by the incident ultraviolet beam. Prominently, the bulk effect of the photocatalytic reaction achieved in the first 10 minutes, see the figure 4.18.

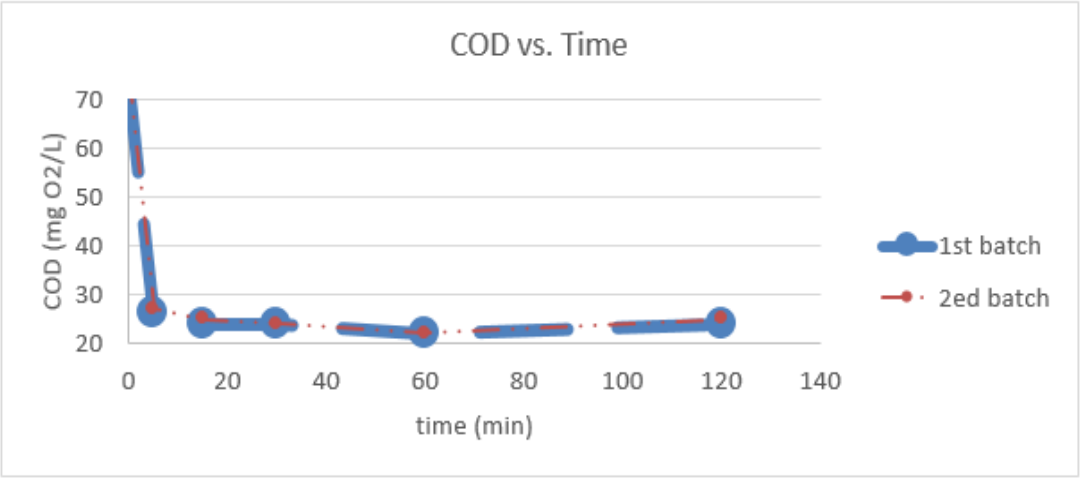


Figure 4.18: Batch experiment for 0.25 mg ZnO catalysis in 100 ml of secondary waste water from Nablus western WWTP.

The remained COD could be atributed to one of the next two reasons: 1) treated ww contains polutants that have band gap energy highr or close to

the zinc oxide's band gap energy of 3.2 eV (Dimapilis et. al, 2018). Thus the produced radecals don't have sufficient energy to degrade these polutants 2) WW could contains antioxidant like phenolic compounds which could preak or Impedes the oxidation cycle in the photocatalytic reaction. At trace concentration, It could hinder photo degredation of complex polutants with higher band gap energy (Al-Saidi et al., 2016).

5.4.2. Nano zinc oxide produced from commercial Micro-Zinc Oxide

The photo degradation ability of zinc oxide produced from micro-sized zinc oxide was tested using 0.25 g ZnO catalysis in 100 ml of the secondary effluent. The experiment was conducted in duplicate simultaneously. Similar to the results of the nano zinc oxide which produced previously, COD of the secondary effluent declined rabidly under the influence of the photo catalytic reactions which was activated by the incident ultraviolet beam. The new powder achieved higher photo degradation efficiency (more than 85%) see figure 4.19. Photo degradation reaction for the commercial based powder took approximately the same activation period for the batch of high purity powder, see section 5.3.1.

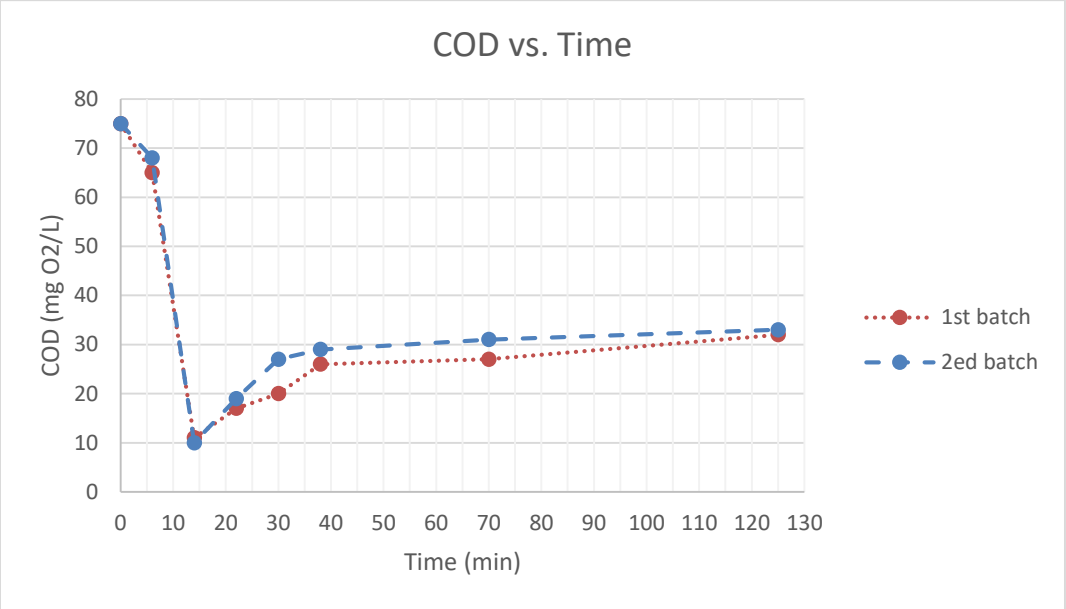


Figure 4.19: Batch experiment for 0.25 g of ZnO catalysis produced from commercial micro-sized ZnO in 100 ml of secondary waste water from Nablus western WWTP**.**

The COD value for increased after reaching its lowest value. This rise doesn't reflect a real COD scince the zinc oxide is believed to be reduced and releas the oxygen atom forming Zn^{++} cataion; because of photo-corrosion of the ZnO photo catalysis under the effect of the incident UV's photons it could releas the oxygen atom to the solution in the batch reactor, the next equation describe the photo-corrosion effect

$$ZnO + 2\,h^{+} \underset{UV}{\rightarrow} Zn^{2+} + \frac{1}{2}O_2$$

The resulting Zn^{2+} is resbonsible for the apearing fake COD (Hongbo et al., 2008), since it will combine with the dicromate in the test kit reflecting the exess COD , see the next eqeaution.

$$Cr_2O_7{}^{2-} + Zn^{2+} \overset{\Delta}{\rightarrow} Zn\,Cr_2O_7$$

The next figure illustrates the Zn^{2+} effect in the batch experiment and the expected COD pattern neglecting the effect of zinc cation.

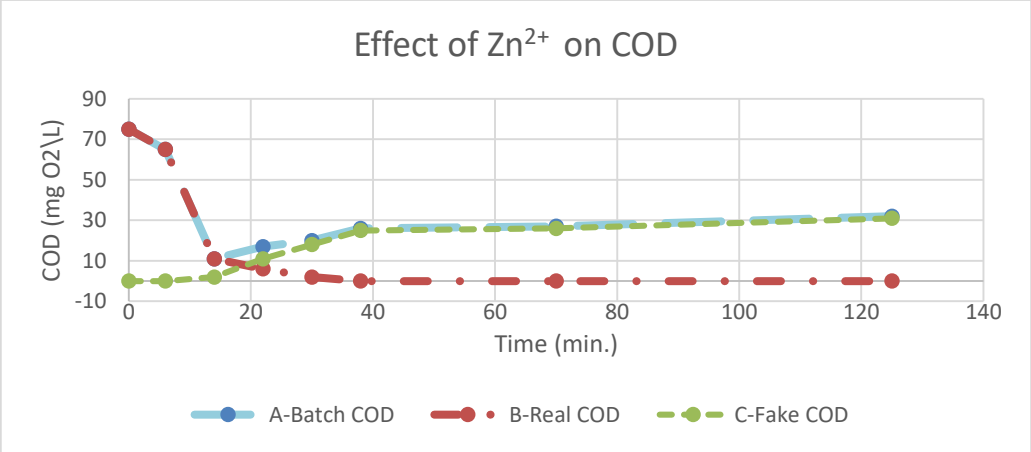


Figure 4.20: The expected effect of Zn^{2+} on COD of the batch experiment, a) ongoing pattern, b) Real pattern neglecting Zn^{2+} effect, c) interpretative effect of the Zn^{2+}.

4.4.3. Nano zinc oxide pre-deposited on the surface of activated carbon

The produced zinc oxide from micro-sized ZnO was predeposited on the surface of the synthesised activated carbon and tested for the photodegradetion ability in batch experemment. The next table showes the deposition yield of four activated carbon samples.

Table 7: Nano ZnO catalysts deposition yield for four activated carbon samples

Modification	AC1	AC2	AC3	AC4
Weight of naked AC (g)	1.0023	1.00051	1.00271	1.00329
Weight of ZnO added (g)	0.4998	0.50203	0.50193	0.50051
Weight of A.C/ZnO after calcination at 200 c for 1hr (g)	1.17088	1.14593	1.13591	1.17321
Weight of ZnO deposited on the AC (g)	0.16858	0.14542	0.1332	0.16992
ZnO deposited %	34 %	29 %	27 %	34 %
Average %	31 ± 4 %			

The average yield in the adopted pre-deposition process was 31±4 % which indecates; two thirds of the used nano photo catalysis in pre-deposition process were not used and should be recycle to achieve the maximum exploitation.

Indeed, COD-batch didn't show a clear results because of the micro corroded patecils of AC which releasd to the WW in the batch reactor due to mexing, causing high and not relevent COD. In the other hand, AC should not has significant interference in exemination of polluutents with direct photometric detection method like methyl orange (Sanna et al., 2016), orange acid (Margan and Haghighi, 2018) and reactive Blue (Habibi and Mardani, 2015).

AC corroded particles are believed to affect the COD test by giving a higher fake values. At the same time, AC/ZnO system is believed to achieve a good photocatalytic behavior (Amer, 2012) but still less effective than the naked ZnO or glass supported catalysis because of the

role of UV and AC in deoxygenation and production of Zn^{2+} and Zn^{3+} anions (Samanta and Jena, 2012)

Moreover, activated carbon as other black solid materials are not permeable for UV spectrum as well as it absorb all the UV light spectrum without reflecting or passing through its rigid particles. This could affects the final application of the filtration media of AC doped with NPC, where the incident UV light just actives the photo catalytic reaction at the surface of the top layer of AC without activating the NPC in-depth porosity or layers ; see figure 4.21.

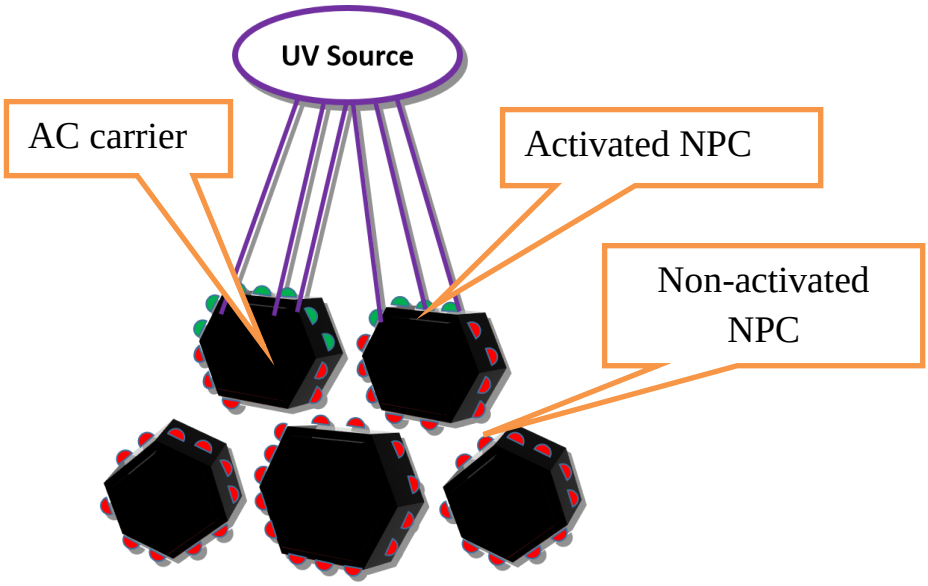


Figure 4.21: UV absorption at the surface AC particles, green semi-spheres represent the activated NPC and the red one represent not activated NPC due to obstruction of UV beams.

4.4.4. Nano zinc oxide pre-deposited on the surface of recycled glass (Glass-ZnO system)

Unlike activated carbon, glass could pass the visible light spectrum and wide range of UV spectrum which makes it as a good candidate for the self-cleaning filtration media. The high permeability and low adsorption of the glass allow the UV radiation to reach the pre-deposited nano photo catalysis in depth of the modified glass media with lowest level of obstruction.

Pre-depositing of NPC on the surface of crushed glass achieved highest yield of 99.5 %, where approximately all of the pre-deposited NPCs were thermally attached to the Underdevelopment glass filtration media without any considerable losses.

glass\ ZnO system achieve the highest COD-removal efficacy of 97 % (figure 4.22). Notably the activation time of the NPC is greater than the activation time of the naked nano powders in the previous batch experiments, this could be attributed to the smaller surface area of the crushed glass.

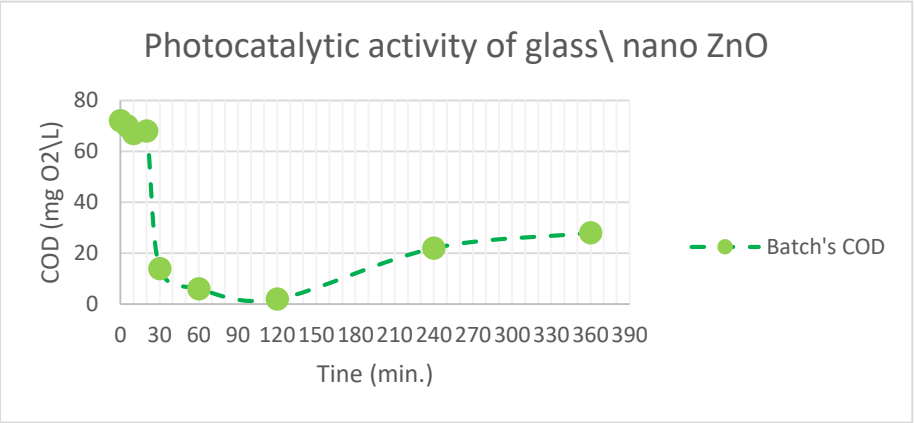


Figure 4.22: Photocatalytic activity of G\ nano ZnO (5:1 weight ratio). Each batch contains 1 g of Glass\ZnO particles and 100 ml of secondary WW effluent.

The rise in the COD value after reaching its lowest value is attributed to the same reason which was discussed in the section 5.3.2.

Conclusion and recommendations

Conclusions

The main conclusions for this research are:

1. Activated carbon usually considered as good option for tertiary wastewater treatment but it couldn't be used as support for the produced nano photocatalysis (NPC) in this research, due to (i) instability of the NPC on its surface, (ii) effect of carbon in acceleration of the deoxygenation process of the doped zinc oxide, and (iii) impermeability of AC for the light spectrums which are required for photocatalytic reaction activation.
2. Nano Zinc oxide could be produced from cheap raw materials with commercial-purity rather than graded raw chemicals like micro-size ZnO and zinc sulfate heptahydrate with no significant difference in the catalysis size.
3. The produced nano photo catalysis showed a good promising photo degradation ability with removal efficiency of COD exceeds 95% for the secondary effluent of Nablus treatment plant during contact time of 10-20 minutes in batch run.
4. The photocatalytic activity was increased after doping the NPC on the surface of the recycled glass, since, the removal efficiency exceeded 97% of the COD in batch experiments containing secondary effluent of Nablus's western wastewater treatment plant.

Recommendations

As a recommendation for future work the below are suggested:

1. Co-doping of the produced nano ZnO with silver could achieve better removal efficacy and more stable catalysis against the observed deoxygenation proclivity.
2. Confined bed is preferable in the final application of the innovated filtration media rather than the traditional loose filtration beds.
3. Despite of permeability of the glass, filtration media shouldn't be deep since deeper medias obstruct the activating light beams.
4. In this research, the used glass for the filtration media is crashed glass with sharp edges. According to the known headloss formula; using more rough glass particles could develop lower headloss in the filtration media.
5. Reuse treated effluents of most of the waste water treatment plants in Palestine is not recommended due to the low quality of the produced effluents.
6. Decision makers should construct tertiary treatment facilities in the Palestinian wastewater treatment plants to enable the reuse of the treated effluents.
7. The continuation of this research requires a serious attention from the University of An-Najah to support the researchs of nanotechnology, where the necessary examination equipment are not available at the university, what costs the students a lot of time and efforts in addition to the relatively high finance costs.

References

- Alaya, M. N., Hourieh, M. A., Youssef, A. M., & El-Sejariah, F. (January 01, 2000). ***Adsorption Properties of Activated Carbons Prepared from Olive Stones by Chemical and Physical Activation***. **Adsorption Science & Technology**, 18, 27-42.
- Alslaibi, T. M., Abustan, I., Ahmad, M. A., & Abu, F. A. (December 01, 2012). ***Effect of Different Olive Stone Particle Size on the Yield and Surface Area of Activated Carbon Production***. **Advanced Materials Research**, 626, 126-130.
- Alslaibi, T. M., Abustan, I., Azmier, M., Foul, A. A., & 2012 International Conference on Advanced Materials Engineering and Technology, ICAMET 2012. (January 24, 2013). ***Effect of different olive stone particle size on the yield and surface area of activated carbon production***. **Advanced Materials Research**, 626, 126-130.
- Amer, H. (2012), **ZnO nano-particle catalysts in contaminant degradation processeswith solar light-Naked and supported systems**- (thesis), An-Najah National University-Nablus-Palestine.
- Ameta, R., & Ameta, S. C. (2017). **Photocatalysis: Principles and applications**, Boca Raton, FL, ISBN: 13: 978-1-4822-5493-8.
- Ansari R. and Mohammad-Khah, A. (2009) ***Activated Charcoal: Preparation, characterization and Applications: A review article***, **International Journal of ChemTech Research**, ISSN: 0974-4290.
- APHA (2005**) Standard Methods for the Examination of Water and Wastewater Analysis**. APHA-AWWA-WEF, Washington DC.

- ASTM standards C 135, 2003, **Standard Test Method for True Specific Gravity of Refractory Materials by Water Immersion**. ASTM international, West Conshohocken, PA 19428-2959, United States.
- ASTM standards D 1252-B, 2006, **Standard Test Methods for Chemical Oxygen Demand (Dichromate Oxygen Demand)**. ASTM international, West Conshohocken, PA 19428-2959, United States.
- ASTM standards D2862, 2010, **Standard Test Method for Particle Size Distribution of Granular Activated Carbon**. ASTM international, West Conshohocken, PA 19428-2959, United States.
- Babakhouya N., S. Boughrara, & F. Abad. (2010). ***Kinetics and Thermodynamics of Cd(II) Ions Sorption on Mixed Sorbents Prepared from Olive Stone and Date Pit from Aqueous Solution***. **Science Publications**.
- Bader, Najoua & Souissi, Souad & Ouederni, Abdelmottaleb. (2014). ***A Controlled Nitric Acid Oxidation of an Olive Stones- based Activated Carbon: Effect of Oxidation Time***. **Lignocellulose**. 3. 22-36.
- Bandosz, T. J. (2006). **Activated carbon surfaces in environmental remediation**. Amsterdam: Elsevier.
- Bansode, R. R., Losso, J. N., Marshall, W. E., Rao, R. M., & Portier, R. J. (January 01, 2003). ***Adsorption of volatile organic compounds by pecan shell- and almond shell-based granular activated carbons***. **Bioresource Technology: Biomass, Bioenergy, Biowastes,**

Conversion Technologies, Biotransformations, Production Technologies, 90, 2, 175-184.

- Berger, Christina. (2012). Biochar and activated carbon filters for greywater treatment: **comparison of organic matter and nutrients removal**. SLU/Dept. of Energy and Technology.
- Çeçen, F. & Aktaş, O. (2012). **Activated carbon for water and wastewater treatment: Integration of adsorption and biological treatment**. Weinheim, Germany: Wiley-VCH.
- Chorkendorff, I., & Niemantsverdriet, J. W. (2017). **Concepts of modern catalysis and kinetics**, Weinheim, Germany, Wiley.
- Davis, M. L. (2010). ***Water and wastewater engineering: Design principles and practice***. New York: McGraw-Hill.
- Dias, J. M., Alvim-Ferraz, M. C. M., Almeida, M. F., Rivera-Utrilla, J., & Sánchez-Polo, M. (January 01, 2007). ***Waste materials for activated carbon preparation and its use in aqueous-phase treatment: A review***. **Journal of Environmental Management**, 85, 4, 833-846.
- Dimapilis, E. A. S., Hsu, C.-S., Mendoza, R. M. O., & Lu, M.-C. (March 01, 2018). ***Zinc oxide nanoparticles for water disinfection***. **Sustainable Environment Research**, 28, 2, 47-56.
- **EPA**, Environmental Protection Agency, Ireland. (1995), **Water Treatment Manuals "Filtration"**, Wexford, Ireland.
- **FAO**, Food and agriculture organization of the united nation and **(WHO)** world health organization joint Expert Committee on Food

Additives, **Compendium of food additive specifications** (2010). 73ed meeting. Rome. ISBN: 978-92-5-106662-1.

- Garland, C. W., Nibler, J. W., & Shoemaker, D. P. (2009). **Experiments in physical chemistry**. Boston: McGraw-Hill Higher Education.
- Ghazi. Y. M Al-Nour (2009) **Photocatalytic Degradation of Organic Contaminants in the Presence of Graphite-Supported and Unsupported ZnO Modified with CdS Particles** (thesis), Palestine: An-Najah National University,P: 132.
- Gupta, V. K., Agarwal, S., Saleh, T. A., Siddiqui, M. N., & Ali, I. (January 01, 2013). ***Chromium removal from water by activated carbon developed from waste rubber tires***. **Environmental Science and Pollution Research**, 20, 3, 1261-1268.
- Haydar, S., Ferro-García, M. A., Rivera-Utrilla, J., & Joly, J. P. (January 01, 2003). ***Adsorption of p-nitrophenol on an activated carbon with different oxidations***. **Carbon**, 41, 3, 387-395.
- Inglezakis, V., & Poulopoulos, S. (2006). **Adsorption, Ion Exchange and Catalysis: Design of Operations and Environmental Applications**. Burlington: Elsevier.
- Jaouadi, M., Hbaieb, S., Guedidi, H., Reinert, L., Amdouni, N., & Duclaux, L. (November 01, 2017). ***Preparation and characterization of carbons from β-cyclodextrin dehydration and from olive pomace activation and their application for boron adsorption***. **Journal of Saudi Chemical Society**, 21, 7, 822-829.

- Johar, M. A., Afzal, R. A., Alazba, A. A., & Manzoor, U. (January 01, 2015). ***Photocatalysis and Bandgap Engineering Using ZnO Nanocomposites***. **Advances in Materials Science and Engineering**, 2015, 1-22.
- Juárez-Galán, J. M., Silvestre-Albero, A., Silvestre-Albero, J., & Rodríguez-Reinoso, F. (January 01, 2009). ***Synthesis of activated carbon with highly developed "mesoporosity"***. **Microporous and Mesoporous Materials**, 117, 519-521.
- Khoshhesab,Z. M., Sarfaraz, M. & Houshyar, Z. (2012) ***Influences of Urea on Preparation of Zinc Oxide Nanostructures Through Chemical Precipitation in Ammonium Hydrogencarbonate Solution***, **Synthesis and Reactivity in Inorganic, Metal-Organic, and Nano-Metal Chemistry**, 42:10, 1363-1368.
- Kumar, S. S., Venkateswarlu, P., Rao, V. R., & Rao, G. N. (January 01, 2013). Synthesis, ***characterization and optical properties of zinc oxide nanoparticles***. **International Nano Letters**, 3, 1, 30.
- Lafuente B, Downs R T, Yang H, Stone N, 2015, ***The power of databases: the RRUFF project. In: Highlights in Mineralogical Crystalography, Walter de Gruyter GmbH***, **Link: http://rruff.info/zincite/display=default/R050419.**
- Lens, P. N. L., Virkutyte, J., Jegatheesan, V., Kim, S.-H., & Al-Abed, S. R. A. (2013). **Nanotechnology for water and wastewater treatment.** London; New York: IWA Publishing, e-ISBN: 978-1-7804-0459-2.

- Martínez, M. L., Torres, M. M., Guzmán, C. A., & Maestri, D. M. (January 01, 2006). ***Preparation and characteristics of activated carbon from olive stones and walnut shells***. **Industrial Crops and Products**, 23, 1, 23-28.
- Martins, A. C., Pezoti, O., Cazetta, A. L., Bedin, K. C., Yamazaki, D. A. S., Bandoch, G. F. G., Asefa, T., Almeida, V. C. (January 15, 2015). ***Removal of tetracycline by NaOH-activated carbon produced from macadamia nut shells: Kinetic and equilibrium studies***. **Chemical Engineering Journal**, 260, 291-299.
- Moreno-Castilla, C., Carrasco-Marin, F., Lopez-Ramon, M. V., & Alvarez-Merino, M. A. (January 01, 2001). ***Chemical and physical activation of olive-mill waste water to produce activated carbons***. **Carbon**, 39, 9, 1415.
- Nouri, H. & Ouederni, A. (2013). ***Modeling of the Dynamics Adsorption of Phenol from an Aqueous Solution on Activated Carbon Produced from Olive Stones***. **International Journal of Chemical Engineering and Applications**. 254-261. 10.7763/IJCEA.2013.V4.306.
- Nuhu Dalhat Mu'azu, Nabel Jarrah, Mukarram Zubair, & Omar Alagha. (September 01, 2017). ***Removal of Phenolic Compounds from Water Using Sewage Sludge-Based Activated Carbon Adsorption: A Review***. **International Journal of Environmental Research and Public Health**, 14, 10, 1094.

- Otero, M., Rozada, F., Calvo, L. F., García, A. I., & Morán, A. (April 01, 2003). ***Elimination of organic water pollutants using adsorbents obtained from sewage sludge***. **Dyes and Pigments**, 57, 1, 55-65.
- Prachi, Gautam, P., Madathil, D., & Brijesh, N. A. N. (September 09, 2013). ***Nanotechnology in waste water treatment: A review***. **International Journal of Chemtech Research**, 5, 5, 2303-2308.
- **PWA** Palestinian water authority **(**2014) **National strategy for water and waste water**.
- **PWA** Palestinian water authority **(**2012) **Annual status report on water resources, water supply, and wastewater in the Occupied State of Palestine**.
- Samhan S, Al-Sa'ed R, Assaf K, Friese K, Afferden M, Muller R, Tumpling W, Ghanem M, Ali W, and Zimmo O, 2010, Wastewater Management Overview in the Occupied Palestinian Territory, Chapter 10: P 229-248, **Waste Water Treatment and Reuse in the Mediterranean Region**, Springer Berlin Heidelberg, ISBN: 9783642182815.
- Sanna, V., Pala, N., Alzari, V., Nuvoli, D., & Carcelli, M. (January 01, 2016). ***ZnO nanoparticles with high degradation efficiency of organic dyes under sunlight irradiation***. **Materials Letters**, 162, 257-260.
- Solar, C., Sardella, F., Deiana, C., Lago, R. M., Vallone, A. & Sapag, K. (December 01, 2008). ***Natural gas storage in microporous carbon***

obtained from waste of the olive oil production. **Materials Research**, 11, 4, 409-414.

- Tchobanoglous, John Crittenden, Rhodes Trussell, David Hand and Kerry Howe (2012). **MWH's Water Treatment: Principles and Design,** 3rd Edition, P 1920, (Tchobanoglous, 2012).
- Ubago-Pérez, R., Carrasco-Marín, F., Fairén-Jiménez, D., & Moreno-Castilla, C. (June 20, 2006). ***Granular and monolithic activated carbons from KOH-activation of olive stones***. **Microporous and Mesoporous Materials**, 92, 64-70.
- **WBCSD** World Business Council for Sustainable Development, 2005, **Water Facts and Trends**.
- Wirasnita, R., Hadibarata, T., Yusoff, A. R. M., Yusop, Z., & Yusoff, A. R. M. (October 01, 2014). ***Removal of Bisphenol A from Aqueous Solution by Activated Carbon Derived from Oil Palm Empty Fruit Bunch***. **Water, Air, and Soil Pollution**, 225, 10.
- Yaghmaeian, K., Khosravi, M. R., Nasseri, S., Mahvi, A. H., Alimohammadi, M., & Nazmara, S. (January 01, 2015). ***Removal of inorganic mercury from aquatic environments by multi-walled carbon nanotubes***. **Journal of Environmental Health Science & Engineering**, 13.
- Youssef A. M., Th. El-Nabarawy and E. I. El-Shafey (2006) Modified ***Activated Carbons from Olive Stones for the Removal of Heavy Metals***, **Carbon Science**, Vol. 7, No. 1 March 2006 pp. 1-8.

- Yuliusman, ., Nasruddin, ., Sanal, A., Bernama, A., Haris, F., & Ramadhan, I. T. (February 01, 2017). ***Preparation of activated carbon from waste plastics polyethylene terephthalate as adsorbent in natural gas storage***. **Iop Conference Series: Materials Science and Engineering**, 176, 12055.
- Zyoud, A., Nassar, H. N. I., El-Hamouz, A., & Hilal, H. S. (April 01, 2015). ***Solid olive waste in environmental cleanup: Enhanced nitrite ion removal by ZnCl2-activated carbon***. **Journal of Environmental Management**, 152.
- Schneider, C. A.; Rasband, W. S. & Eliceiri, K. W. (2012***), "NIH Image to ImageJ: 25 years of image analysis"***, ***Nature methods*** **9 (7)**: 671-675, PMID 22930834 (on Google Scholar).
- Rahman, I., Saad B., Shaidan S., & Syarizal E. (September 01, 2005). ***Adsorption characteristics of malachite green on activated carbon derived from rice husks produced by chemical–thermal process***. **Bioresource Technology**, 96, 14, 1578-1583.
- Bernardo E.C., Egashira R.. & Kawasaki J., (January 01, 1997). ***Decolorization of molasses' wastewater using activated carbon prepared from cane bagasse***. **Carbon**, 35, 9, 1217-1221.
- El-Hamouz, A., Hilal, H. S., Nassar, N., & Mardawi, Z. (January 01, 2007). ***Solid olive waste in environmental cleanup: oil recovery and carbon production for water purification***. **Journal of Environmental Management**, 84, 1, 83-92.

- Huang, Y., Sun, Y., Xu, Z., Luo, M., Zhu, C., & Li, L. (January 01, 2017). ***Removal of aqueous oxalic acid by heterogeneous catalytic ozonation with MnOx/sewage sludge-derived activated carbon as catalysts***. **Science of the Total Environment**, 575, 50-57.
- Uğurlu, M., Kula, I., Karaoğlu, M. H., & Arslan, Y. (December 01, 2009). ***Removal of Ni(II) ions from aqueous solutions using activated-carbon prepared from olive stone by ZnCl activation***. **Environmental Progress & Sustainable Energy**, 28, 4, 547-557.
- Lin, Y.-R., & Teng, H. (July 01, 2002). ***Mesoporous carbons from waste tire char and their application in wastewater discoloration***. **Microporous and Mesoporous Materials**, 54, 167-174.
- Molina-Sabio, M., & Rodriguez-Reinoso, F. (January 01, 2004***). Role of chemical activation in the development of carbon porosity***. **Colloids and Surfaces. A, Physicochemical and Engineering Aspects**, 241, 1, 15.
- Alhamed, Y. (January 01, 2006). ***Activated Carbon from Dates' Stone by ZnCl2 Activation***. **Journal of King Abdulaziz University-Engineering Sciences**, 17, 2, 75-98.
- Choi, K. J., Kim, S. G., Kim, C. W., & Park, J. K. (May 01, 2006). ***Removal efficiencies of endocrine disrupting chemicals by coagulation/flocculation, ozonation, powdered/granular activated carbon adsorption, and chlorination***. **Korean Journal of Chemical Engineering**, 23, 3, 399-408.

- Mianowski, A., Owczarek, M., & Marecka, A. (July 01, 2007). ***Surface Area of Activated Carbon Determined by the Iodine Adsorption Number***. **Energy Sources, Part A: Recovery, Utilization, and Environmental Effects**, 29, 9, 839-850.
- Hongbo, Fu., Xu, T., Zhu, S., & Zhu, Y. (November 01, 2008). ***Photocorrosion Inhibition and Enhancement of Photocatalytic Activity for ZnO via Hybridization with C60***. **Environmental Science and Technology**, Washington Dc-, 42, 21, 8064-8069.
- Jiao, Li., Y., Yang, Z., & Gao, N. (January 01, 2009). ***Regeneration of nano-ZnO photocatalyst by the means of soft-mechanochemical ion exchange method***. **Journal of Environmental Sciences**: Supplement 1, 21.
- Samanta, D., & Jena, P. (May 23, 2012). ***Zn in the +III Oxidation State***. **Journal of the American Chemical Society**, 134, 20, 8400-8403.
- Chokshi, N.P., Bora, L , (March-2014), ***An Overview of Nanotechnology in Waste Water Treatment, Resource recovery, water reuse and recycle for sustainable development*** (Conference Paper).
- Habibi, M. H., & Mardani, M. (February 25, 2015). ***Co-precipitation synthesis of nano-composites consists of zinc and tin oxides coatings on glass with enhanced photocatalytic activity on degradation of Reactive Blue 160 KE2B***. **Spectrochimica Acta Part A: Molecular and Biomolecular Spectroscopy**, 137, 785-789.

- Al-Saidi, I. A.-D. H. A., & Sadik, F. (January 01, 2016). ***Synthesis and Investigation of Phenol Red Dye Doped Polymer Films***. **Advances in Materials Physics and Chemistry**, 6, 5, 120-128.
- Yakout, S. M., & Sharaf, E.-D. G. (January 01, 2016). ***Characterization of activated carbon prepared by phosphoric acid activation of olive stones***. **Arabian Journal of Chemistry**, 9.
- Zhang, C., Tang, J., Peng, C., & Jin, M. (September 01, 2016). ***Degradation of perfluorinated compounds in wastewater treatment plant effluents by electrochemical oxidation with Nano-ZnO coated electrodes***. **Journal of Molecular Liquids**, 221, 1145-1150.
- Bohli, T., Ouederni, A., Fiol, N., & Villaescusa, I. (January 01, 2015). ***Single and binary adsorption of some heavy metal ions from aqueous solutions by activated carbon derived from olive stones***. **Desalination and Water Treatment**, 53, 4, 1082-1088.
- Margan, P., & Haghighi, M. (January 01, 2018). ***Sono-coprecipitation synthesis and physicochemical characterization of CdO-ZnO nanophotocatalyst for removal of acid orange 7 from wastewater***. **Ultrasonics - Sonochemistry**, 40, 323-332.
- Fujishima, A. K. I. R. A., & Honda, K. E. N. I. C. H. I. (July 01, 1972). ***Electrochemical Photolysis of Water at a Semiconductor Electrode***. **Nature**, 238, 5358, 37-38.
- Butt, S. B., Innayat, M., Riaz, M., & Mahmood, A. (January 01, 1998). ***Activated carbon from scrap tires for water purification***. **Wedc Conference**, 24, 340-342.

جامعة النجاح الوطنية
كلية الدراسات العليا

"التنقية المتقدمة للمياه العادمة باستخدام الفلترة المعتمدة على تكنولوجيا مواد النانو"

إعداد
أحمد الخالدي

إشراف
د. عبد الفتاح حسن
أ.د. عامر الهموز

قدمت هذه الأطروحة استكمالا لمتطلبات الحصول على درجة الماجستير في هندسة المياة والبيئة بكلية الدراسات العليا في جامعة النجاح الوطنية في نابلس، فلسطين.

2018

"التنقية المتقدمة للمياه العادمة باستخدام الفلترة المعتمدة على تكنولوجيا مواد النانو"

إعداد

أحمد الخالدي

إشراف

د. عبد الفتاح حسن

أ.د. عامر الهموز

الملخص

تحظى مشكلة المياه باهتمام شديد على الصعيد العالمي، حيث ان نقص موارد المياه العذبة وازدياد نسبة التلوث في المياه الجوفية والسطحية حث صانعي القرار على تبني تقنيات معالجة المياه الحديثة. في فلسطين هناك تشجيع لسياسة اعادة استخدام المياه العادمة المعالجة في الري وحقن المياه الجوفية و لكن جودة المياه المعالجة المنتجة في محطات الوطن لا تناسب المعايير الصارمة لإعادة استخدام المياه العادمة.

كحل لمشكلة عدم ملائمة جودة المياه المعالجة في المحطات الفلسطينية تم اقتراح تحديث الفلاتر التقليدية باستخدام مواد متوفرة ورخيصة وهي حفاز الزنك من مقياس النانو متر، بحيث يوفر ذلك فلاتر ذات وقت تشغيل اطول من المعتاد و اقل حاجة للشطف العكسي للفلتر مما يجعل عملية الفلترة اكثر ديمومة وجدوى.

في هذه الدراسة تم انتاج اكسيد الزنك من مقياس النانو باستخدام مواد ذات نقاوة عالية (99.5%) وباستخدام مواد ذات جودة تجارية بنقاوة 95% ولم يلاحظ فرق كبير في حجم الحفازات المنتجة بناءً على جودة المواد الخام المستخدمة. حيث تم انتاج اكسيد الزنك بمقياس 29 نانو من كبريتات الزنك سباعية الماء عالي النقاوة كما وتم انتاجه من كبريتات الزنك سباعية الماء ذات الجودة التجارية بقياس 69 نانو. وبنمط مشابه تم انتاج اكسيد الزنك من اكسيد الزنك ذو النقاوة التجارية بقياس المايكرو بقياس 28 نانو بزيادة بسيطة لا تتجاوز 11 نانو عن اكسيد الزنك المنتج من اكسيد الزنك ذو النقاوة العالية بقياس المايكرو.

تم فحص قدرة مواد النانو المنتجة على التحليل الضوئي للملوثات الموجودة في المياه العادمة المعالجة حيث تم الفحص باستخدات مواد النانو بصورة بودرة "مسحوق" او بعد الصاقها على الفحم المنشط او الزجاج المسحوق. احرزت تجارب الكفاءة لمواد النانو بصورة البودرة معالجة بمقدار 85% لعبء الملوثات معبرا عنه بتركيز الأوكسجين اللازم لأكسدة تلك الملوثات. كما واحرزت تجارب الكفاءة للزجاج المدموج مع مواد النانو نسبة معالجة تصل الى 97% علما ان مواد النانو منتجة من المواد الخام ذات الجودة التجارية .

تم فحص الكربون المنشط والزجاج كحامل لحفازات النانو المنتجة ولم يحقق الفحم الغاية المنشودة حيث لوحظ سهولة انفلات مواد النانو عن سطح الفحم المنشط اضافة لعدم نفاذية الفحم للاشعة الضوئية اللازمة لتنشيط التفاعلات الضوئية اللازمة لتحليل الملوثات. وعلى نقيض الفحم ابدت حبيبات الفلتر المصنوعة من الزجاج المدموج مع مواد النانو ثباتية لمواد النانو الملصقة وقابلية لتمرير الضوء اللازم لتنشيط التفاعلات الضوئية. ختاما، نتائج هذا البحث تعد حجر الاساس للبحوث التالية لغاية انتاج فلتر ذاتي التنظيف.